Fire Performance of Modular Wall Panels: Numerical Analysis

Dilini Perera

Faculty of Engineering and Environment, University of Northumbria, Newcastle, UK

K. Poologanathan

Faculty of Engineering and Environment, University of Northumbria, Newcastle, UK

P. Gatheeshgar

Faculty of Engineering and Environment, University of Northumbria, Newcastle, UK

I. R. Upasiri

Department of Civil Engineering, University of Sri Jayawardenepura, Sri Lanka

P. Sherlock

ESS Modular, Crag Ave, Clondalkin Industrial Estate, Dublin 22, Ireland

H. Rajanayagam

Faculty of Engineering and Environment, University of Northumbria, Newcastle, UK

B. Nagaratnam

Faculty of Engineering and Environment, University of Northumbria, Newcastle, UK

Abstract

The Modular Building System (MBS) is increasingly popular and promoted due to the inherent advantages over conventional construction. Fire performance of a building has become a crucial design consideration because of the recent detrimental fire accidents. However, for modular buildings, there has been less previous evidence of research on the fire performance. Investigations become necessary since double skin wall and floor modular panel systems are involved in MBS in contrast to conventional buildings. Therefore, this work investigates the fire performance of Light-gauge Steel Framed (LSF) modular wall panels with different configurations through numerical analyses. Heat transfer numerical models were developed and validated against the full-scale fire test results comparing the time-temperature response. The validated numerical models were subsequently extended to analyse the fire performance of conventional and modular LSF wall panels. This includes 16 modular wall configurations with single and double fire resistance plasterboard linings and three different insulations, namely rock wool, glass fibre and mineral wool. The structural fire resistance time was determined using the established Load Ratio (LR) vs critical Hot-Flange (HF) temperature correlation. The results demonstrated that there is no noticeable difference in the structural fire resistance time between the modular and the corresponding mapped conventional LSF wall configurations. However, modular wall panels experience enhanced insulation fire resistance up to 170% for single-lined plasterboards and up to 80 % for double-lined plasterboard configurations. The analysis also yields that there is no significant influence of the choice of insulation material between rock-wool, glass-fibre and mineral-wool on structural fire resistance.

Keywords: Modular Wall, Numerical Studies, Load Ratio versus Critical Temperature, FRL, Fire Performance, Light-gauge Steel Frame, Standard Fire

1 Introduction

Modular Building System (MBS), specifically the constructions involving volumetric MBS units is an emerging construction technique employed all over the world in recent times. The popularity of this construction technique is due to its inherent advantages over conventional construction methods. The advantages include high productivity, high quality, reduced project timeline, less generation of waste, cost-efficiency and reduced noise generation [1-3]. Due to these potential advantages, MBS is promoted in the UK especially as a viable solution to the housing crisis [4-6]. Besides, MBS can be used for several building applications such as commercial, educational, residential and health care infrastructures. A volumetric MBS unit may consist of load bearing or non-load bearing Light-gauge Steel Framed (LSF) wall panels, floor panels and ceiling panel. Such volumetric units being assembled together to make impressive structures is the current practice. Therefore, the internal wall panels of the construction are formed with two LSF wall panels contributed from the two volumetric MBS units on either side. Even though MBS has certain promising advantages the link to how it performs under fire is still not understood comprehensively.

However, the fire performance of conventional LSF buildings is quite well understood and still, research studies are underway to further improve the fire performance of LSF wall and floor components. LSF wall and floor panels are made of light gauge steel channels (frame assembly), fire resistance board linings, and insulation in between light gauge steel channels or external insulation. The intention to control the temperature rise in the light gauge steel channels is that the strength properties deteriorate with temperature in light gauge steel; thus, reduce the load-carrying capacity. Fire performance of LSF wall and floor panels were investigated with respect to channel section type such as lipped channel, hollow flange and web stiffened channels [7-9], fire resistance board type including gypsum plasterboard, calcium silicate boards, and magnesium oxide boards [10-16], and type of insulation materials such as rock wool, glass fibre, cellulose fibre. Moreover, the effect of changing the location of the insulation materials has also been investigated [17]. Some other research and investigations [18-21] on modular and conventional LSF construction have focused on the structural behaviour of those cold-formed steel structures under seismic loading conditions. Simultaneously, extensive experimental fire performance studies conducted on clod-formed steel structures [22-25] have been the initiative step for more specific investigative studies in this research scope. Also, staggered slotted perforations can be incorporated to light gauge steel channels to enhance the fire and thermal performance, however, the reduction of the structural capacity of the member due to openings should be considered [26-28]. Overall this method is a good option to be incorporated in modular buildings for enhanced thermal performance [29]. Based on the finding appropriate design methods were proposed in the aforementioned research studies to design the LSF panels considering fire aspects. However, these kinds of detailed investigations were not performed for the modular building panels. When it comes to internal wall panels of the Modular Building System, two volumetric units stacked back-to-back results in double skin LSF wall panel as shown in Figure 1 extracted from Lawson [30]. The current industry practice doesn't consider this double skin nature of the LSF wall panels, hence, the structural, integrity and insulation FRLs are specified for the single skin wall panels only. In such an incident, the actual FRLs would be considerably higher than what is specified. Hence, the proper understanding on FRLs of internal modular wall panel is necessary for the effective use of material over the conservative approach used in the industry. Figure 2 shows the general internal wall arrangements of a conventional LSF wall panel and a modular LSF wall panel as reported by Lawson [31].

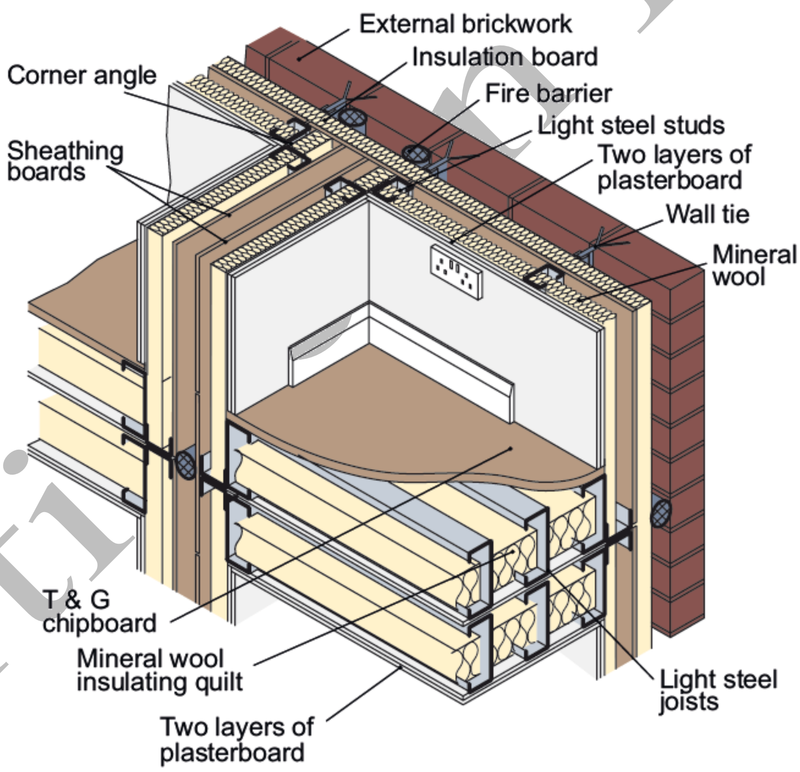

Figure 1: Typical LSF wall/ floor arrangement of a Modular Building System (MBS) [30]

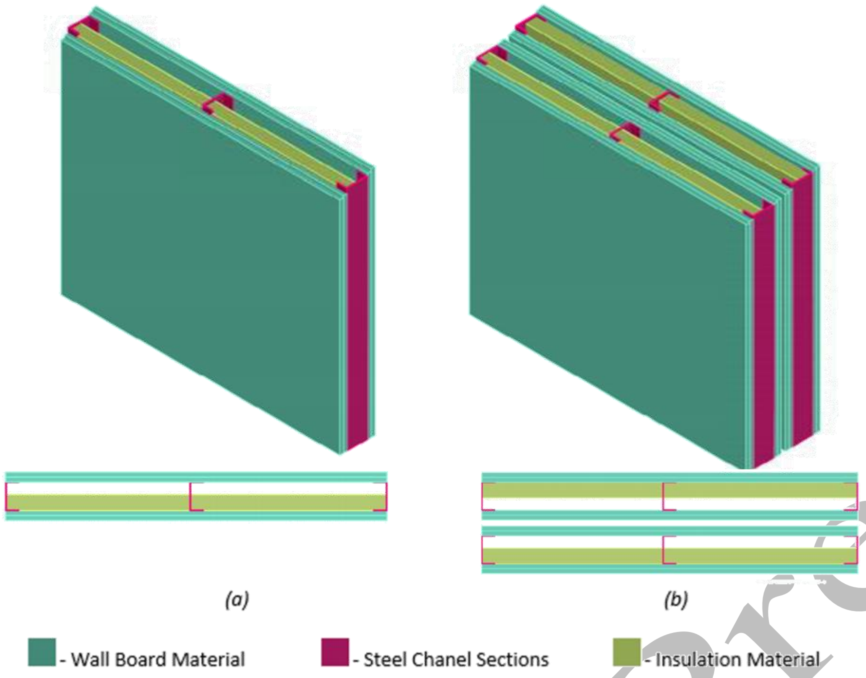

Figure 2: Typical wall configurations of; (a): conventional LSF wall panel & (b) modular LSF wall panel

Fire assessment of MBS is paramount as the consequences are severe in terms of fatal accidents and property damage. Further, the recent fire accident of 100-bedroom Moorfield hotel, a multi-story modular construction project has highlighted the attention towards to fire performance consideration of the buildings. During the recent Moorfield hotel fire accident residents and staff members escaped safely [32]. This is a modular construction that consisted of Oriented Strand Board (OSB) wall panels and combustible polyurethane insulation [33]. Figure 3 shows the fire accident of the Moorfield hotel. Thus, all emerging construction of steel-frame MBS also needs to be investigated for its fire performance to ensure adequate time to evacuate the occupants safe.

Figure 3: Fire accident of Moorfield hotel [32, 33]

Hence, despite of all inherent strengths of LSF and modular construction techniques, it is quite necessary to address the susceptibility to catastrophic failure of these cold-formed steel structures under fire scenarios. With the absence of knowledge on fire performance of different configurations of modular LSF walls under fire, this study has been conducted incorporating several parameters based on the industry practice on conventional and modular LSF wall panels under standard fire condition. Therefore, this paper presents details on fire performance analysis of steel-framed modular wall panels using numerical studies and the analysis. The validity of the numerical models was ensured comparing the time-temperature profiles obtained from fire tests and numerical models. The validated heat transfer models were then extended to analyse the fire performance of modular LSF wall panels. A parametric based analysis of modular LSF wall panels was performed considering different wall configurations including different wallboard linings (single and double fire resistance plasterboard linings), two different plasterboard thicknesses (12.5 mm and 15 mm), and different types of insulation materials (rock wool, glass fibre, and mineral wool). These parameters have been carefully selected based on the practices of modular construction industry in UK and European countries. The results were then compared with mapped conventional LSF wall configuration to compare the effect of double skin nature of modular LSF walls. The fire-resistance rating of modular LSF wall panels is presented and discussed herein.

2 Understanding of Modular Building System Fire Safety

Although often recognized as fire rating, the correct term used in standards and gudelines for defining the building element's fire resistance is FRL (Fire Resistance Level). The FRL reflect a building element's ability to sustain fire for a specified period of time under testing conditions, and is expressed as a measure of structural adequacy, integrity, and then insulation [34]. For instance 60 minutes FRL of a load-bearing wall can be indicated as 60/60/60 where structural, integrity and insulation fire resistances are presented respectively. Structural adequacy is known as the ability of a load-bearing element to support the specified load, under fire conditions. In general, this is vital for load-bearing wall systems. Secondly, integrity is the member's capacity to avoid the passage of flames and hot gasses. Next insulation is the ability to maintain the unexposed surface temperature rises below the critical temperatures (i.e.: 140 ^{0}C on average and 180 ^{0}C at any location) [35].

Standards around the world, AS 1530: Part 4 [36], ISO 13784-1 [37] , BS EN 13501 [38] and AISI design provisions [39] use the standard fire time-temperature curve to obtain the FRL of building elements. Several recent research studies have revealed that the maximum temperature of a natural fire surpassed the standard fire time-temperature curve in a short period from ignition [40-43] as shown in Figure 4. However, the standard fire curve has been adopted in this study so that the FRLs of the novel wall specimens can be easily compared against that of the conventional panels.

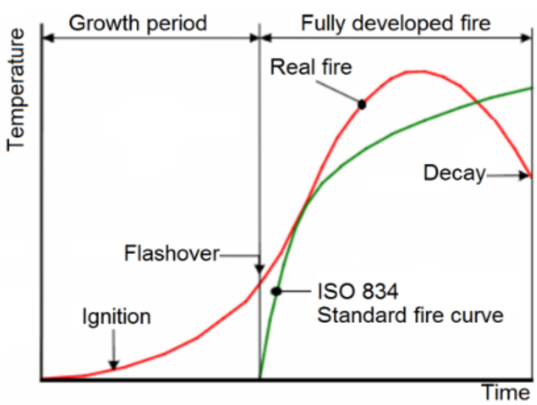

Figure 4: Comparison of real fire and standard fire ISO 834 [43]

For the structural fire designs of steel structures, the advanced calculation models in Eurocode 3 [44] can be adapted, but the LSF walls studied here were made of composite structures which, besides cold-formed steel studs, consist of various types of plasterboards and insulation materials. Hence, it should be noted that the simplified models from such standards and guidelines alone, cannot be used to determine FRL of LSF walls. And furthermore, a finite element model for a similar LSF panel that was tested in full scale testing with standard fire has to be established to implement structural fire design and analyses of conventional and modular LSF wall panels. Among experimental investigations available on LSF wall fire behaviour, the full scale fire tests conducted by Gunalan et. al [45] and Magarabooshanam et. al [46], have been numerically modelled and validated in this study. These FEMs have been then extended to study the 24 parametric wall components.

Moreover, studying the full scale fire test results and coupled structural-thermal analyses of LSF walls by Gunalan and Mahendran [47], Chen et. al [48], Gunalan [49] and Ariyanayagam and Mahendran [50], correlation between the applied Load Ratio (LR) and the critical Hot Flange (HF) temperature of the wall stud could be understood. This relationship has been described in more details in section 4.1 and this correlation has been adopted in the study to evaluate the structural adequacy of the parametric wall arrangements.

3 Finite Element Analyses of Modular and Conventional LSF wall panels

In this study, the fire resistance of modular and LSF wall arrangements have been investigated where the thickness of the plasterboard, number of plasterboard layers and the cavity insulation option are the selected parameters in this study. Specifically, sixteen modular and eight conventional LSF wall specimens have been studied. Based on UK market availability 12.5 mm and 15 mm thicknesses of gypsum plasterboards have been considered, while 90x42x2 mm channel section has been adopted from Lawson [30] which is the commonly applied channel section in modular LSF wall panels in UK practice. Moreover, the wall specimens have been considered with and without cavity insulation options. Again, taking into account the material availability in the UK construction industry, rock wool, glass fibre and mineral wool insulation options have been considered for the parametric study. Furthermore, the heat transfer results of modular LSF wall panels (those without cavity insulation and with rock-wool insulation) were compared against single skin LSF wall specimens of same dimensions. Figure 5 shows the modular LSF wall specimens considered in the study.

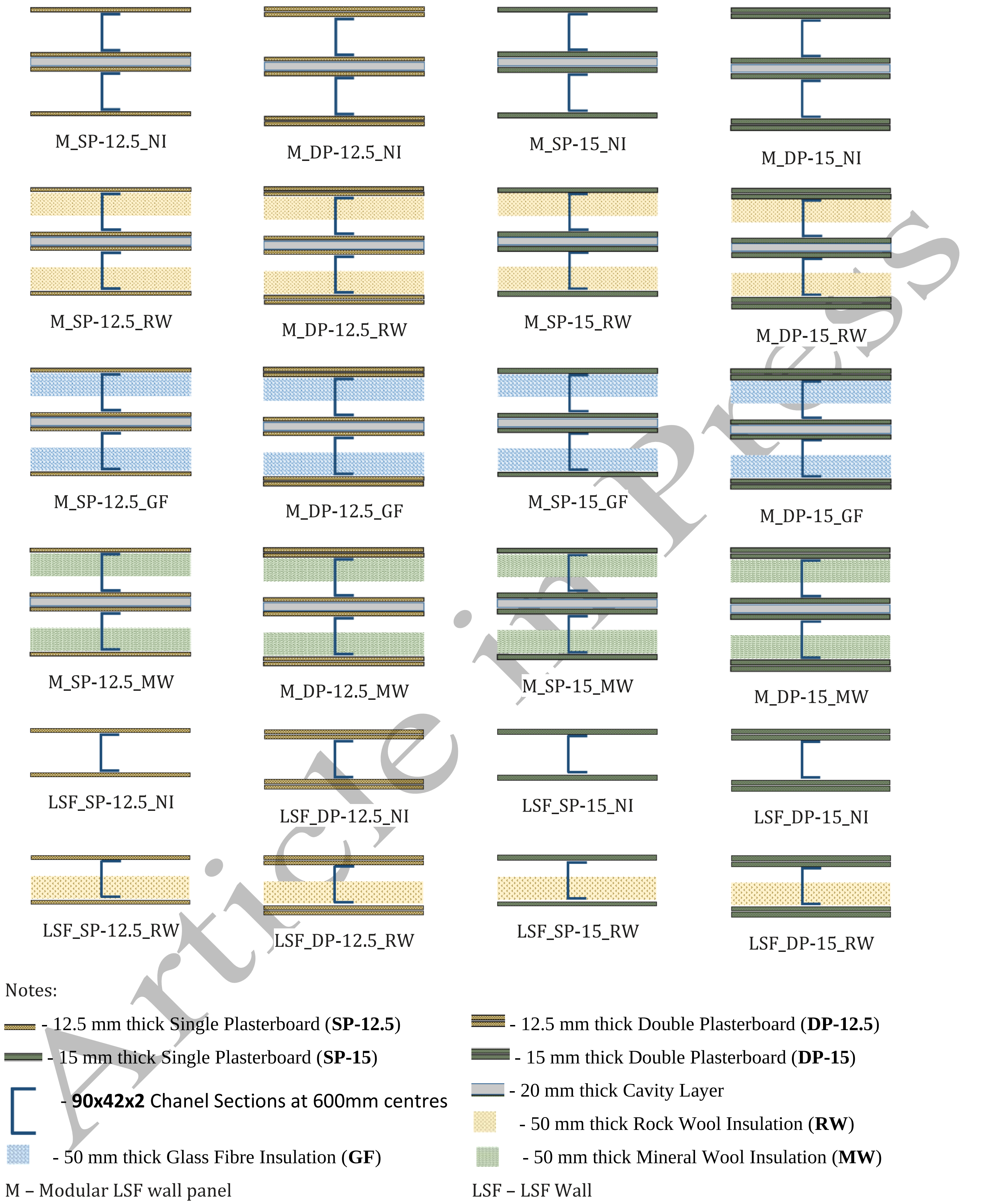

Figure 5: Modular and LSF wall specimens considered in the study

ABAQUS CAE, the commercially available explicit FEA package [51] has been used for the 2D and 3D numerical analyses in this study. Firstly, FEMs were produced for the full scale fire test results available for single and double skin LSF wall configurations so that 2D and 3D Heat Transfer Analyses (HTA) were conducted producing time dependent temperature variation through wall thickness. With the successful validation of the FEA results against the experimental results, those FEMs were extended to model the sixteen modular and eight LSF wall specimens.

3.1 Thermal properties of Modular and Conventional LSF wall panel components

As a building component is subjected to fire, the temperature on fire side increase from ambient temperature to beyond 1100 ^{0}C. Since the thermal properties of most of the building material in the construction industry exhibit a great variation over the subjected temperature, the HTA definitely should make use of elevated temperature thermal properties to produce realistic results. At the same time, the design FRL of LSF or modular LSF wall panel can be even more than 180 minutes where HTA of conventional and modular LSF wall panel configurations are necessary to be conducted over 240 minutes. This prolonged period of exposure to fire temperatures makes it even more essential to consider elevated temperature thermal properties in the HTA.

In order to conduct HTA, the elevated temperature density, thermal conductivity and specific heat of steel, gypsum plasterboard, rock-wool, glass fibre and mineral wool have been extracted from Eurocode 3 [44] and previous studies [52] as presented in Table 1.

Table 1: Elevated temperature thermal properties of wall panel material

Material	Density (kg/m^3)	Thermal Conductivity (W/m.^{0}C)	Specific Heat (J/kg. ^{0}C)
Steel [44]	7850 kg/m^3	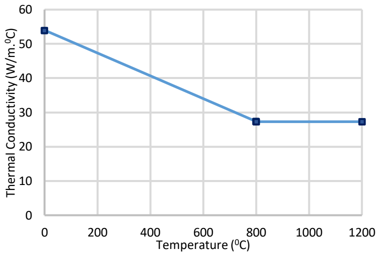	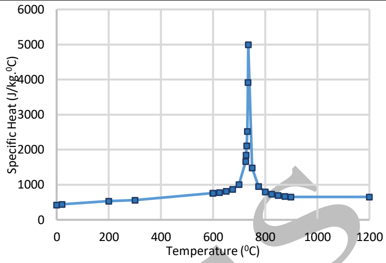
Gypsum Plaster-board [52]	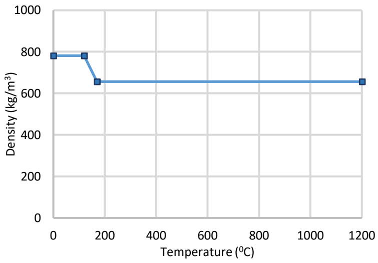	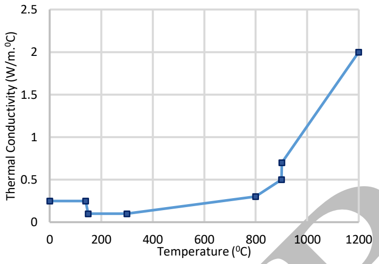	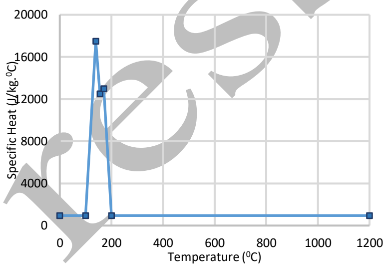
Rock Wool [52]	100 kg/m^3	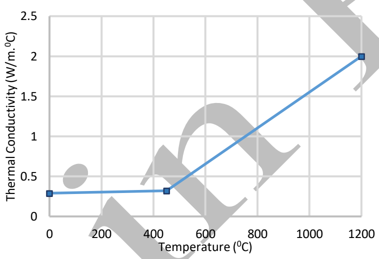	840 J/kg.^{0}C
Glass Fibre [52]	15.42 kg/m^3	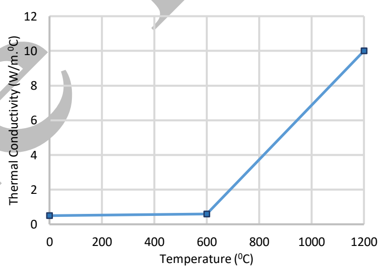	900 J/kg.^{0}C
Mineral Wool [53, 54]	80 kg/m^3	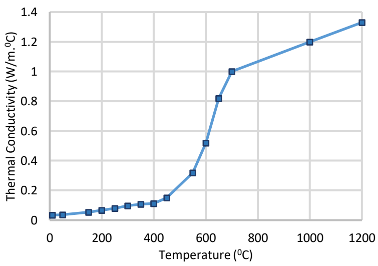	840 J/kg.^{0}C

3.2 FEM Details

When developing the FEMs for the previously experimented conventional LSF wall panels and modular and LSF wall specimens in the parametric study, 1.8 m long wall panels were modeled. However, double skin Conventional LSF wall panel tested by Magarabooshanam et. al [46] was 3m in length and the same length was modeled in the numerical study. The height of walls in 3D FEMs were 0.6m while the wall thicknesses were based on wall cross-section details as presented in Figure 5, Figure 9 and Table 2 for parametric walls, double skin LSF wall and single skin LSF walls respectively.

The global mesh density was 50 mm while 4 mm mesh was applied in the through thickness direction since the temperature distribution and the heat transfer rate in the through thickness direction are much significant compared to the other two directions. The validation results presented in section 3.4 is a verification that the chosen mesh densities are adequate to produce reliable heat transfer analysis results. 3D model of M_SP-15_RW modular LSF wall panel specimen is shown in Figure 6.

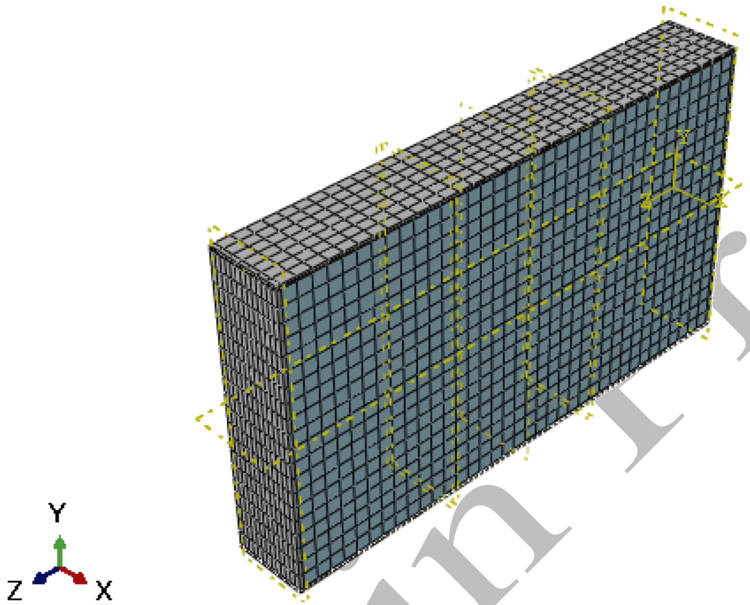

Figure 6: 3D FEM developed for 15 mm thick single plasterboard modular LSF wall panel specimen with rock-wool insulation

The application of finite elements, thermal interactions, constraints and thermal boundary conditions and the use of initial and heat transfer steps in the analyses have been conducted based on previous studies by Keerthan and Mahendran [13] and Rusthi et. al [52]. The above mentioned model details are basically simulate the conduction, convection and radiation mode heat transfer of the building component.

Initially, the LSF or modular LSF wall panel is in ambient temperature before fire accident starts. Therefore, in FEA, an initial step is defined, through which the temperature of the whole model was set to ambient temperature which was 20 ^{0}C in this study. Secondly, a heat transfer step was created as a transient step that is 14400 s long and as it follow the initial step in the analysis. The initial step time was set to 10 s while the minimum and maximum step increments were 0.01 and 100 respectively. The step time was chosen to be automatically calculated so that based on amplitude gradient of fire curve, the software would choose the optimum time step as the analysis progresses. In the initial step, it is not necessary to conduct any HTA, hence no boundary limits or interactions such as convection and radiation was applied for the initial step. On contrary, the heat transfer step was created to simulate the fire accident, hence appropriate boundary conditions and interactions were applied on the model with the produced heat transfer step as illustrated in Figure 7.

When it comes to the application of boundary conditions, standard fire curve, 'ISO 834' [36, 44] time –

temperature amplitude curve was applied on the fire side of the wall, while conduction, convection and radiation mode heat transfer mechanisms have to be progressed in the analysis to produce time – temperature variations at other locations of the wall. Here the conduction mode heat transfer in the model has been enabled in two methods; first ‘DC3D8’ heat transfer brick element available in Abaqus application was applied for all wall components to ensure conduction within each component, then all the surfaces in contacts were restrained in ‘tie constraints’ in Abaqus to facilitate perfect conduction heat transfer from one component to the other in contact. Therefore, the surface interactions between steel studs, insulation material and wall boards have been assigned with tie constrains.

Then the convection and radiation mode heat transfer mechanisms have been enabled applying suitable interactions to the model. Each 3D model of the considered wall specimens consists of 3 cavity surfaces, fire side surface and ambient side surface that involve convection and radiation heat transfer. Among these, convection mode heat transfer inside cavity surfaces can be reasonably neglected as the staged air inside the cavity is trapped in all sides so that the airflow is negligible as explained by Rusthi et al. [52]. Same literature has explained the appropriate surface film coefficients for the fire side and ambient side as 25 W/m.^{0}C and 10 W/m.^{0}C, respectively while the relative emissivity value for radiation heat transfer from all 5 surfaces to be 0.9. To verify the adoption of coefficients and FEA methods from literature, the validation results of five single skin LSF walls and one double skin LSF wall have been presented in section 3.4. When conducting the FEA, the wall panel was covered with plasterboard sections from top and bottom to simulate the covered cavity regions, since practically in the application wall panel does not stand alone with open cavities. Therefore, when applying the cavity radiation interactions, closed cavity method in Abaqus was chosen.

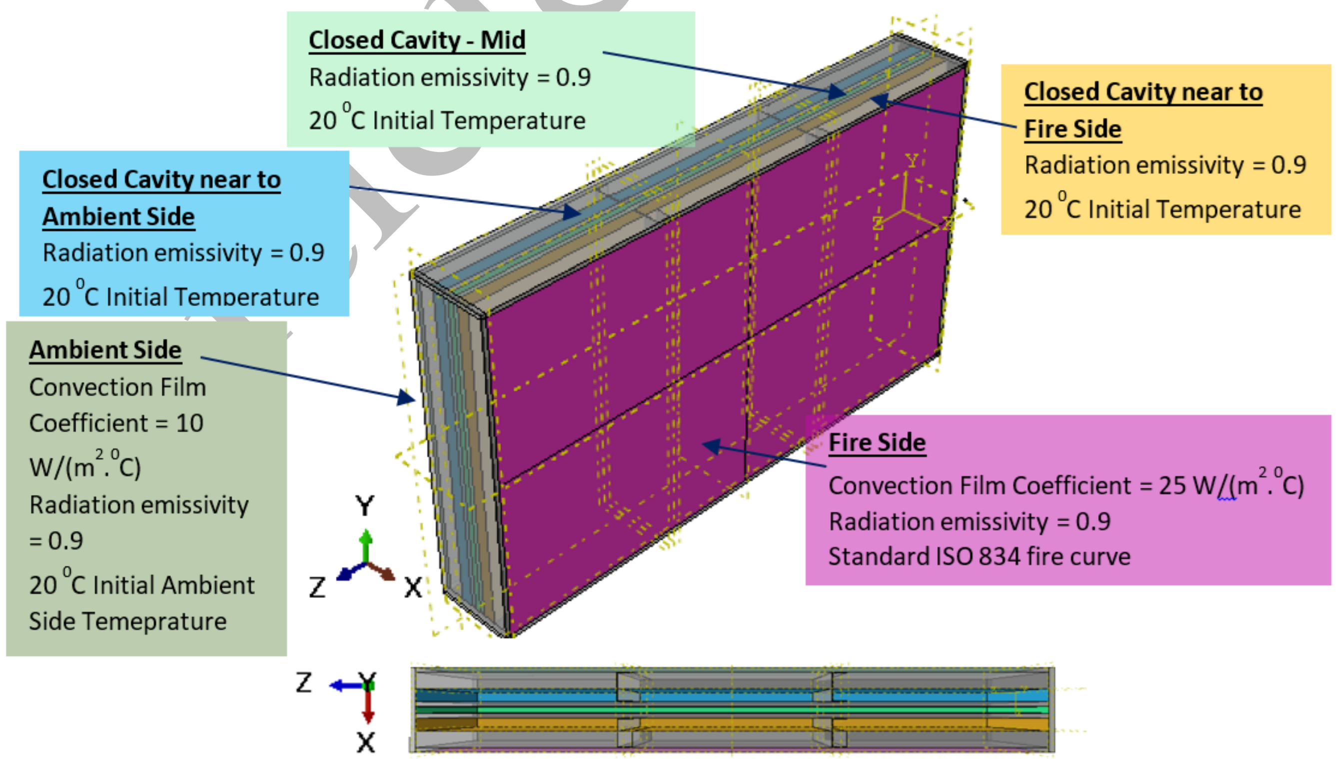

Figure 7: Boundary conditions and interactions on 3D FEM of 15 mm single plasterboard modular LSF wall panel

specimen with rock-wool insulation

The amplitude curve for the standard fire temperature has been presented in equation (1) in ^{0}C;

$$\theta = 345 log_{10}(8t + 1) + 20 \tag{1}$$

where t is the time in minutes [52]. The ambient temperature of 20 ^{0}C has been considered in equation (1).

In Abaqus CAE, the heat flux q on exposed surfaces is calculated as in equation (2) [55];

$$q = h(T_{surf} - T_{sink}) + \sigma\varepsilon\left(\left(T_{surf} - T_{abs}\right)^4 - \left(T_{sink} - T_{abs}\right)^4\right) \tag{2}$$

where T_{surf} is surface temperature, T_{sink} is the sink temperature, T_{abs} is the absolute temperature, h is the convective heat transfer coefficient, ε is the relative emissivity (0.9) and σ is the Steffan-Boltzmann coefficient ($5.67 \times 10^{-8}\ W/(m^2.\text{°C}^4)$). Equation (2) is a combination of convection and radiation mode heat transfer which are the two possible methods of heat transfer from exposed surfaces. Same model is applied for closed cavity surfaces where the first part of the equation is dismissed as convection mode heat transfer inside cavity is negligible with the restricted air flow.

Meanwhile, heat flux for cavity surfaces q_i^c, which is governed by radiation can be expressed in equation (3) [55];

$$q_i^c = \frac{\sigma\varepsilon_i}{A_i}\sum_j \varepsilon_j \sum_k F_{ik} C_{kj}^{-1}\left(\left(T_j - T_{abs}\right)^4 - \left(T_i - T_{abs}\right)^4\right) \tag{3}$$

where A_i is the area of the ith facet seen to all cavity facets of $j = 1,2, \ldots, n$; ε_i and ε_j are the relative emissivity of ith and jth facets. k is again a variable from 1,2,..n; $F_{ik}$and C_{kj} are view factor and reflective matrices while $T_i$are T_j are the temperatures of ith and jth facets.

3.3 Addressing the Limitations of FEA

The main limitation with FEA is the simulation of shrinkage behaviour and crack propagation of plasterboards. Gypsum plasterboards used in the wall specimens are susceptible to lose mass in thin layers when subjected to fire which is known as the Ablation behaviour [56]. Then, heat transfer through the wall specimens would be underestimated. To tackle this problem measured thermal conductivity values had been modified as per previous numerical studies [52] and the modified values have been used in the HTA of this study. Furthermore, integrity criterion FRL has not been evaluated with numerical studies due to the limitations of simulating the crack propagation. Hence, FRL based on integrity criterion has not been evaluated while structural and insulation FRLs have been.

3.4 Validation

As already described in previous sections, full scale fire test results are available for five single skin LSF walls by Gunalan et. al [45] which are shown in Table 2. 3D FEMs were developed for these five wall configurations and the heat transfer analysis results have been graphed against the experimental time dependent temperature variations in Figure 8. The clear agreement between FEA and experimental temperatures of Fire Side (FS), Hot-Flange (HF), Cold-Flange (CF) and Ambient Side (AS) in Figure 8 is a verification of all the FEA methods and parametric values used. Moreover, it should be noted that each wall specimen exhibited excessive deflection of the wall studs leading to structural instability and overall structural failure during the experiments. This is totally due to the increased temperatures of the steel at its HF and the corresponding material property degradation of steel as temperature rises. Therefore, coincidence of experimental and numerical HF temperature profiles indicates the same structural behaviour of the wall studs and the overall wall panel although structural numerical analyses have not been performed in this approach. Hence, FEM development and HTA of modular and LSF wall specimens could be conducted in this order to produce realistic time-temperature curves.

Moreover, HTA has been conducted on a double skin Conventional LSF wall panel presented in Figure 9 which had been tested by Magarabooshanam et. al [46]. The corresponding FEA results against the experimental fire test data have also been presented in Figure 10. With this validation, the FEMs in the study have been further verified.

Table 2: Experimentally tested five single skin LSF wall configurations by Gunalan et. al [45]

Model No:	Wall Cross-Section	Insulation	Plasterboard Arrangement	Failure Time (min)
1		None	Single Board	54
2		None	Double Boards	111
3		Glass Fibre	Double Boards	101
4	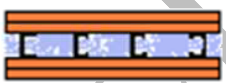	Rock Fibre	Double Boards	107
5		Cellulose Fibre	Double Boards	110

C - 90x40x15x1.15 Lip Channel Section — 16 mm thick Gypsum Plasterboard

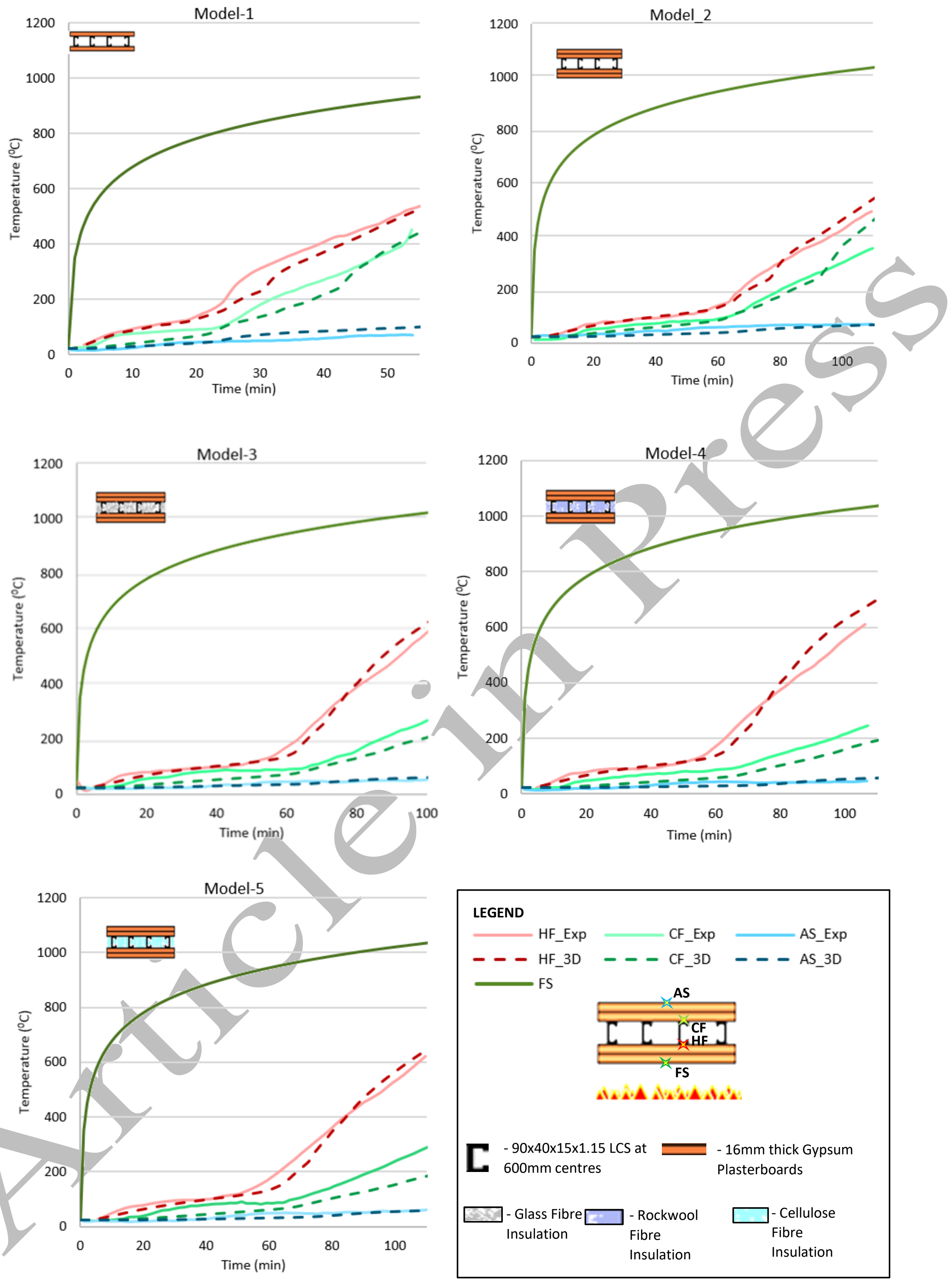

279

280 **Figure 8: Experimental [45] and FEA time-temperature variations through wall thickness for five single skin**

281 **Conventional LSF wall panels**

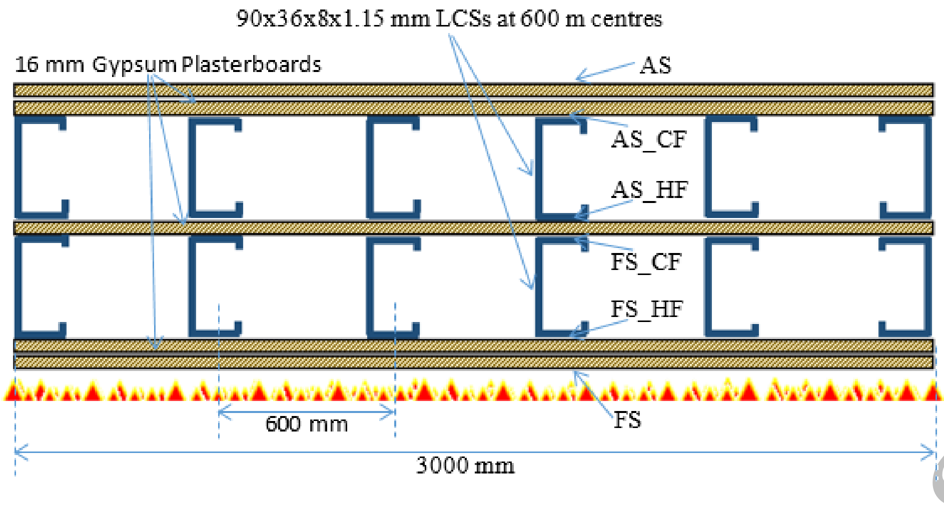

Figure 9: Experimentally tested double skin LSF wall by Magarabooshanam et al. [46]

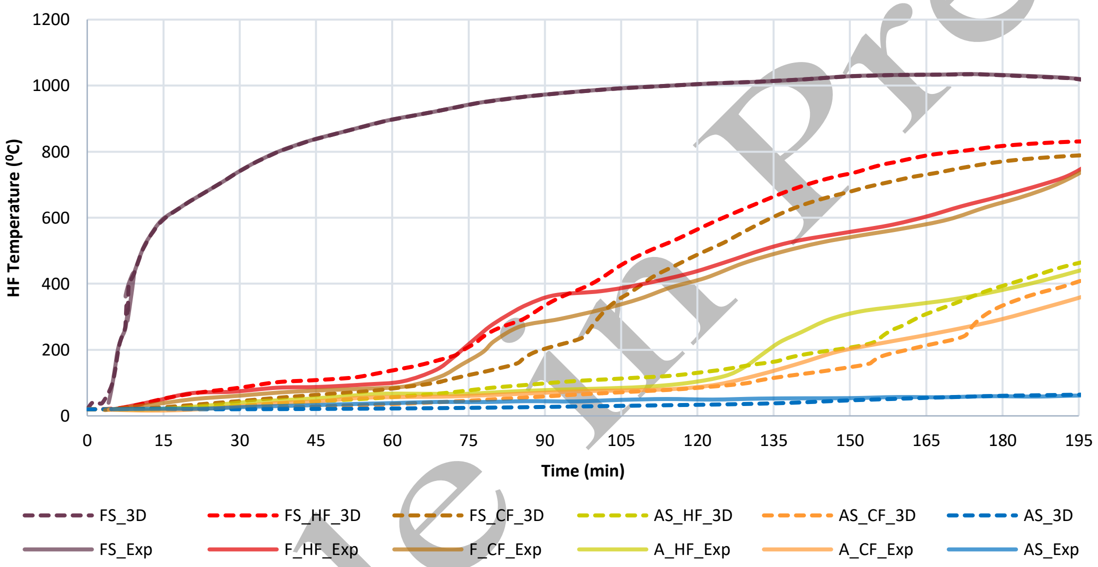

Figure 10: Experimental [46] and FEA time-temperature variations through wall thickness for double skin Conventional LSF wall panel

3.5 Heat Transfer Analyses

2D and 3D HTA have been conducted on sixteen modular and 8 LSF wall specimens presented in Figure 5, while 2D and 3D heat transfer analysis results were almost the same. Figure 11 shows the time – temperature variations of 'M_SP-15_NI' wall derived from 2D and 3D HTA. A graphical presentation of the nodal temperature variation over four hour time period for the same wall panel is presented in Figure 12.

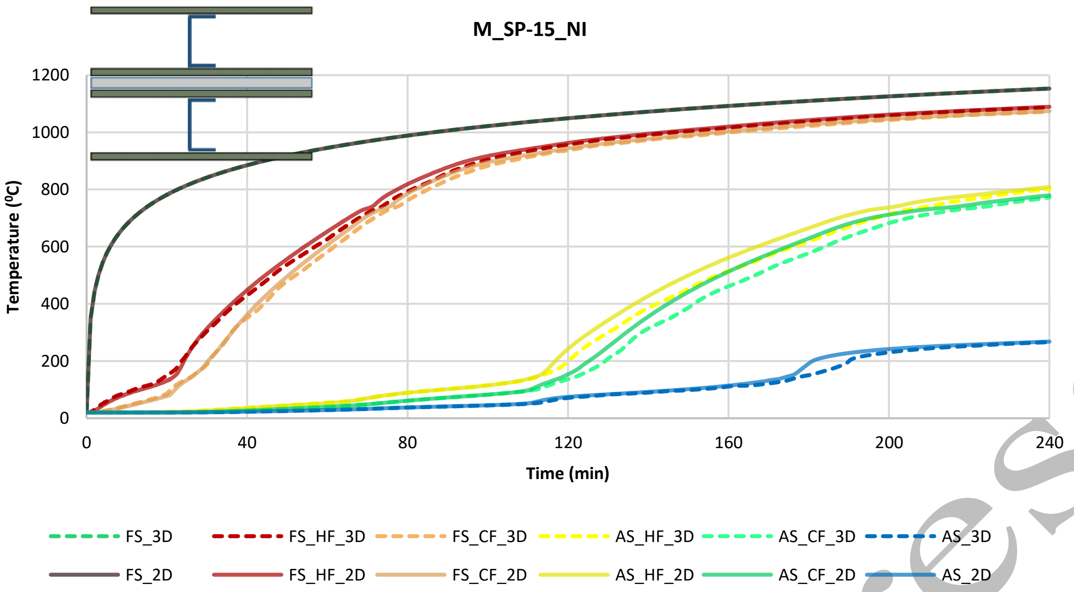

Figure 11: 3D versus 2D FEA results for 15 mm thick single plasterboard modular LSF wall panel specimen with no cavity insulation

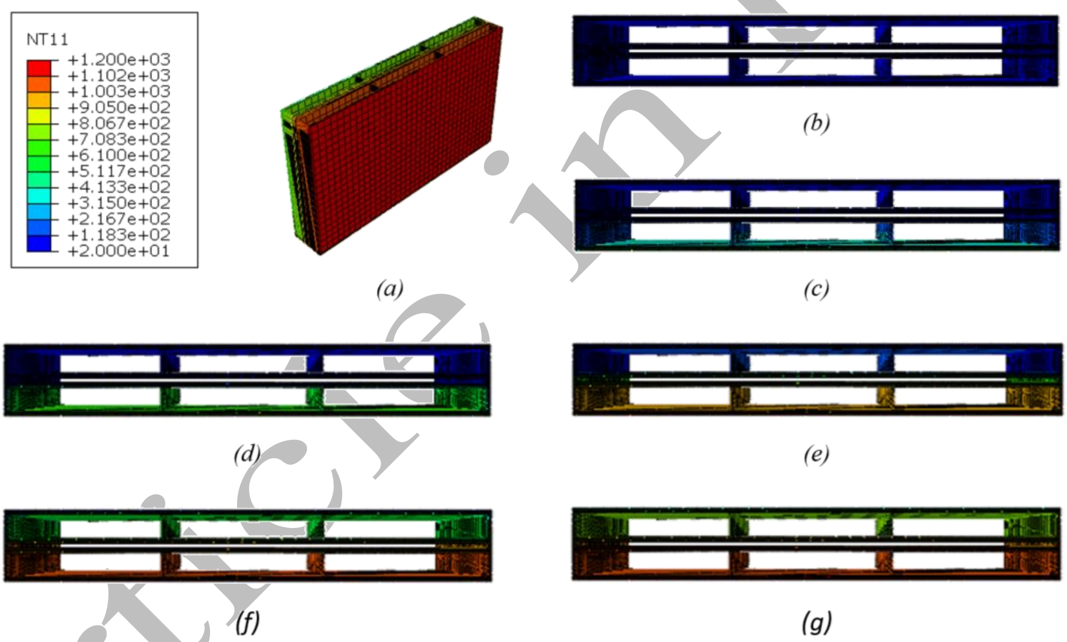

Figure 12: FEA temperature distributions of 15 mm thick single plasterboard modular LSF wall panel specimen with no cavity insulation, (a): 3D view at 4 h and cross-section views at, (b) 0 minutes; (c): 30 minutes; (d): 1 h; (e): 2 h; (f): 3 h and (g) 4 h

Additionally, the results of an insulated wall specimen, ‘M_SP-15_RW’ was also chosen to be presented in Figure 13 and Figure 14.

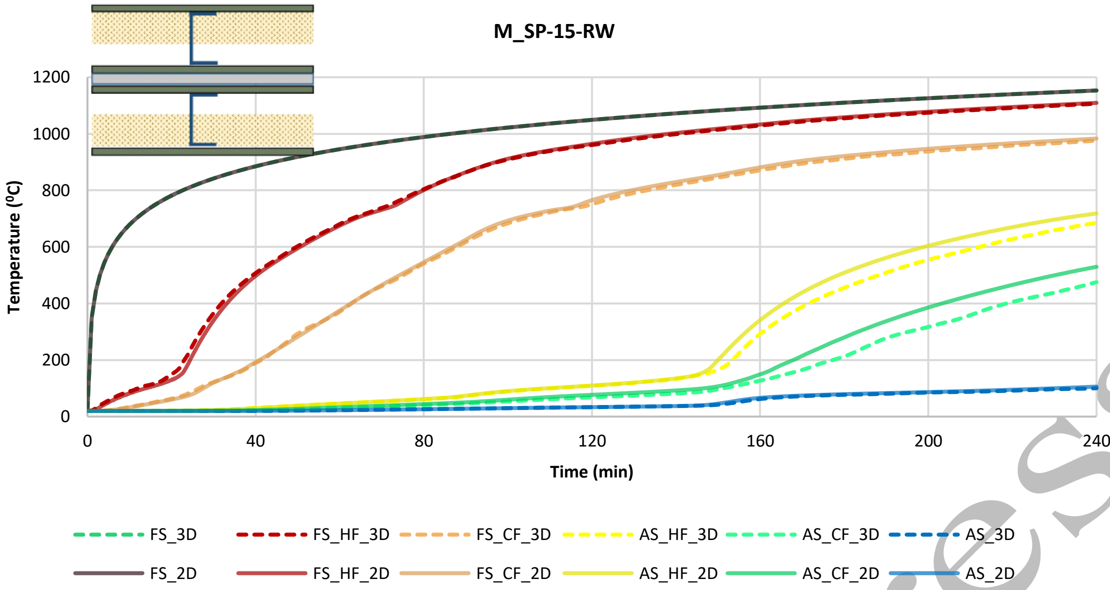

Figure 13: 3D versus 2D FEA for 15 mm thick single plasterboard modular LSF wall panel specimen with rock wool cavity insulation

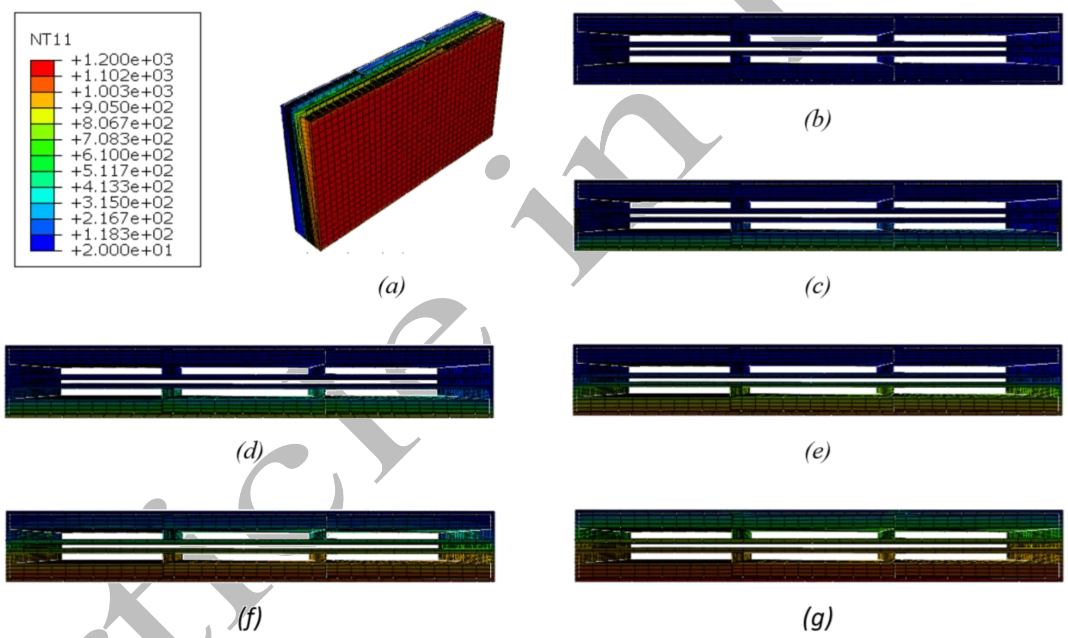

Figure 14: FEA temperature distributions of 15 mm thick single plasterboard modular LSF wall panel specimen with rock-wool cavity insulation, (a): 3D view at 4 h and cross-section views at, (b) 0 minutes; (c): 30 minutes; (d): 1 h; (e): 2 h; (f): 3 h and (g) 4 h

Analysing the 2D versus 3D heat transfer temperature variations, a nice match could be observed, so that it can be could concluded that the 2D heat transfer analysis for Conventional and modular LSF wall panel configurations produce realistic results, where 2D analyses consumes very less analysis time compared to the 3D analyses.

Studying the temperature contours of 'M_SP-15_NI' specimen (with no insulation) against 'M_SP-15_RW' specimen (with rockwool insulation), the temperature gradient through wall thickness at a distinct time has been increased in the insulated wall panel. As insulation material is incorporated in an LSF wall panel, the transfer of heat is blocked by the insulation resulting in accumulation of heat in the HF. This is the reason behind the higher HF temperatures in the insulated modular LSF wall than that of the non-insulated modular LSF wall.

4 Results and Analyses

4.1 Determination of FRL

The FRL of a modular or LSF wall is defined in structural, integrity and insulation criteria. In this study, two approaches have been taken to evaluate structural and insulation FRL of the parametric wall specimens.

Structural FRL:

As explained in section 2, the bearing resistance of cold-formed steel reduces as the thermal properties vary along with increased temperature in fire. Hence, analysing 94 structural fire failure results of LSF wall specimens from full scale fire tests and coupled structural-thermal analyses by Gunalan and Mahendran [47], Chen et. al [48], Gunalan [49] and Ariyanayagam and Mahendran [50], an assertive relationship between applied LR and the critical HF temperature of LSF wall studs can be built-up as shown in Figure 15. The critical HF temperature in Figure 15 is referred to the temperature of HF, when the bearing resistance of the HF reduces beyond the applied mechanical stress on HF at the considered LR. It should be noted that the previously tested LSF walls considered here consist of 1 to 2 mm thick channel sections that are about 90 mm deep, while the fire tests and numerical analyses had been conducted under 'ISO 834', standard fire curve on the fire side of the LSF walls.

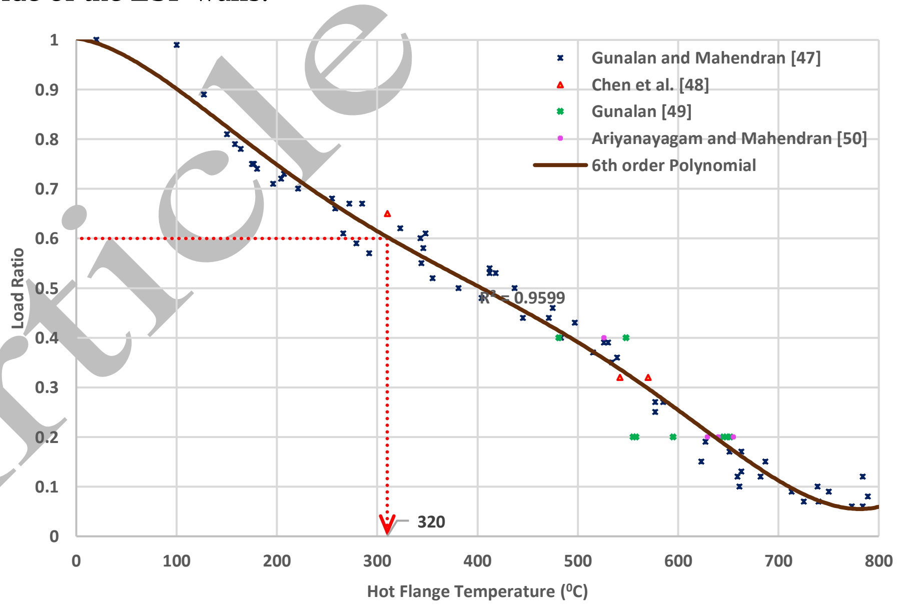

Figure 15: Structural fire failure of LSF walls- LR versus critical HF temperature relationship [47-50]

Using the established model between LR and critical HF temperature, the HF temperature of a LSF or modular LSF wall panel under structural fire failure could be straight away predicted. For instance at 0.6 LR, the critical HF temperature of a LSF wall is determined as 320 ^{0}C as shown in Figure 15. Table presents the critical HF temperatures for LSF wall panel structural failure when the LR vary from 0.2 to 0.8. To read the critical HF temperatures for the LR values between the given values either a linear interpolation or Figure 15 can be used.

Table 3: Critical HF temperatures for structural fire failure at different LRs

LR	0.2	0.3	0.4	0.5	0.6	0.7	0.8	0.9
Critical HF Temperature (^{0}C)	645	570	490	405	320	235	159	77

Likewise, the critical HF temperature for a LSF wall configuration can be determined with respect to the applied LR. Then, to determine the structural FRL of a desired LSF wall panel, HTA can be implemented to estimate the HF temperature variation of that LSF wall under fire. Once the time-temperature graph for the HF of the LSF wall under consideration has been produced, it could be compared with the critical HF temperature value determined firstly so that the time for HF to reach the critical temperature can be estimated as shown in Figure 16. That way the structural FRL of a LSF or modular LSF wall panel specimen could be calculated.

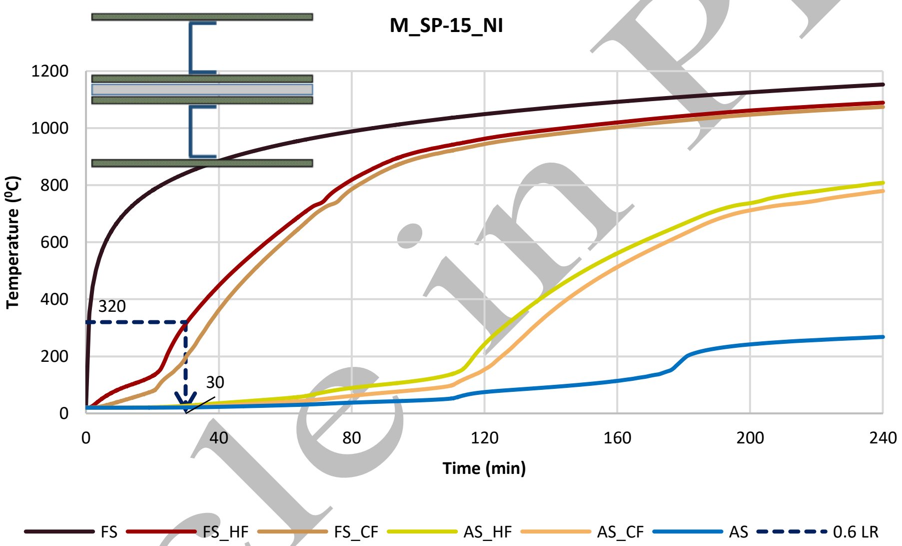

Figure 16: Estimation of structural FRL of 'M_SP-15_NI' modular LSF wall panel specimen at LR = 0.6

The same procedure was followed for LR values from 0.2 to 0.8 and on each HTA of parametric wall specimens as presented in Figure 17 to Figure 20 and tabulated in Table 4 and Table 5. Furthermore, insulation FRL has been estimated in the same heat transfer graphs presented in Figure 17 to Figure 20 and in Table 4 and Table 5.

Table 4: Fire resistance of modular LSF wall specimens based on HTA

Wall Type	Fire Resistance Criteria		Fire Resistance for different Insulation Options (min)			
			NI	RW	GF	MW
M_SP-12.5	Structural	0.2 LR	51	50	47	46
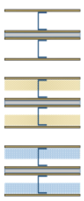		0.3 LR	43	40	38	38
		0.4 LR	35	32	30	30
		0.5 LR	30	27	25	26
		0.6 LR	24	24	22	23
		0.7 LR	20	20	20	20

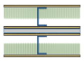		0.8 LR	18	18	17	18
	Insulation		142	>240	173	>240
M_SP-15 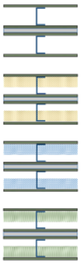	Structural	0.2 LR	60	56	54	54
		0.3 LR	51	47	45	45
		0.4 LR	42	39	37	37
		0.5 LR	37	33	31	33
		0.6 LR	30	29	27	29
		0.7 LR	26	26	24	26
		0.8 LR	25	23	20	23
	Insulation		177	>240	>240	>240
M_DP-12.5 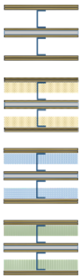	Structural	0.2 LR	88	85	81	81
		0.3 LR	80	75	73	72
		0.4 LR	72	67	64	64
		0.5 LR	64	60	58	60
		0.6 LR	57	55	52	55
		0.7 LR	50	50	49	50
		0.8 LR	45	46	46	46
	Insulation		234	>240	>240	>240
M_DP-15 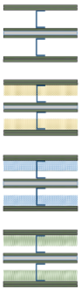	Structural	0.2 LR	105	100	96	95
		0.3 LR	95	90	88	86
		0.4 LR	86	81	79	78
		0.5 LR	78	75	73	73
		0.6 LR	72	68	67	68
		0.7 LR	63	64	62	64
		0.8 LR	60	60	58	59
	Insulation		>240	>240	>240	>240

Notes:

M – Modular LSF wall panel

LSF – Light-gauge Steel Frame Wall

SP – Single Plasterboard

DP – Double PlasterboardLoad Ratio (LR) – The ratio between the applied load on the LSF wall with respect to its load bearing capacity at the ambient temperature

Table 5: Fire resistance of conventional LSF wall specimens based on HTA

Wall Type	Fire Resistance Criteria		Fire Resistance for different Insulation Options (min)	
			NI	RW
LSF_SP-12.5 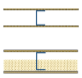	Structural	0.2 LR	51	49
		0.3 LR	43	40
		0.4 LR	35	32
		0.5 LR	28	26

		0.6 LR	23	22
		0.7 LR	20	19
		0.8 LR	16	16
	Insulation		52	82
LSF_SP-15 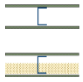	Structural	0.2 LR	60	56
		0.3 LR	50	46
		0.4 LR	42	38
		0.5 LR	35	31
		0.6 LR	29	27
		0.7 LR	25	25
		0.8 LR	20	20
	Insulation		65	95
LSF_DP-12.5 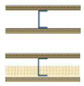	Structural	0.2 LR	90	85
		0.3 LR	80	75
		0.4 LR	70	66
		0.5 LR	62	60
		0.6 LR	56	55
		0.7 LR	50	49
		0.8 LR	43	43
	Insulation		130	165
LSF_DP-15 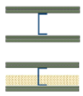	Structural	0.2 LR	107	99
		0.3 LR	97	88
		0.4 LR	86	80
		0.5 LR	78	72
		0.6 LR	70	68
		0.7 LR	62	62
		0.8 LR	58	58
	Insulation		165	203

Notes:

M – Modular LSF wall panel

LSF – Light-gauge Steel Frame Wall

SP – Single Plasterboard

DP – Double PlasterboardLoad Ratio (LR) – The ratio between the applied load on the LSF wall with respect to its load bearing capacity at the ambient temperature

In modular LSF wall panels, critical steel temperature has been considered as the HF temperature of the steel studs that are nearer to the fire exposed side. Although both LSF skins are considered as the load bearing elements, as the steel studs nearer to the FS reaches the critical steel temperature, the stud starts to experience excessive deflection leading the whole wall panel arrangement to go through the overall structural failure.

The use of LR versus critical steel temperature relationship in predicting the structural FRL is in-fact a robust technique although there can be small variations when the loading conditions, stud geometry and sizes vary. However, since LSF wall panel arrangements have been chosen with same stud geometry and axial compression loading arrangements. Hence, the prediction of structural FRLs of the parametric wall panels by analysing the HTA results with respect to the relationship between LR and critical steel temperature is an effective technique.

Insulation FRL:

According to Eurocode 3 [44], the limit for average temperature rise at the unexposed surface of wall to maintain the insulation fire resistance is 140 ^{0}C. Since the ambient temperature considered in the analyses are 20 ^{0}C, the limit for average temperature at the unexposed surface of the wall should remain less than 160 ^{0}C to yield the insulation FRL. Therefore, the time –temperature variation for the unexposed side or the ambient side of the wall was compared against 160 ^{0}C, so that the insulation FRL has been evaluated for all wall specimens considered in the study.

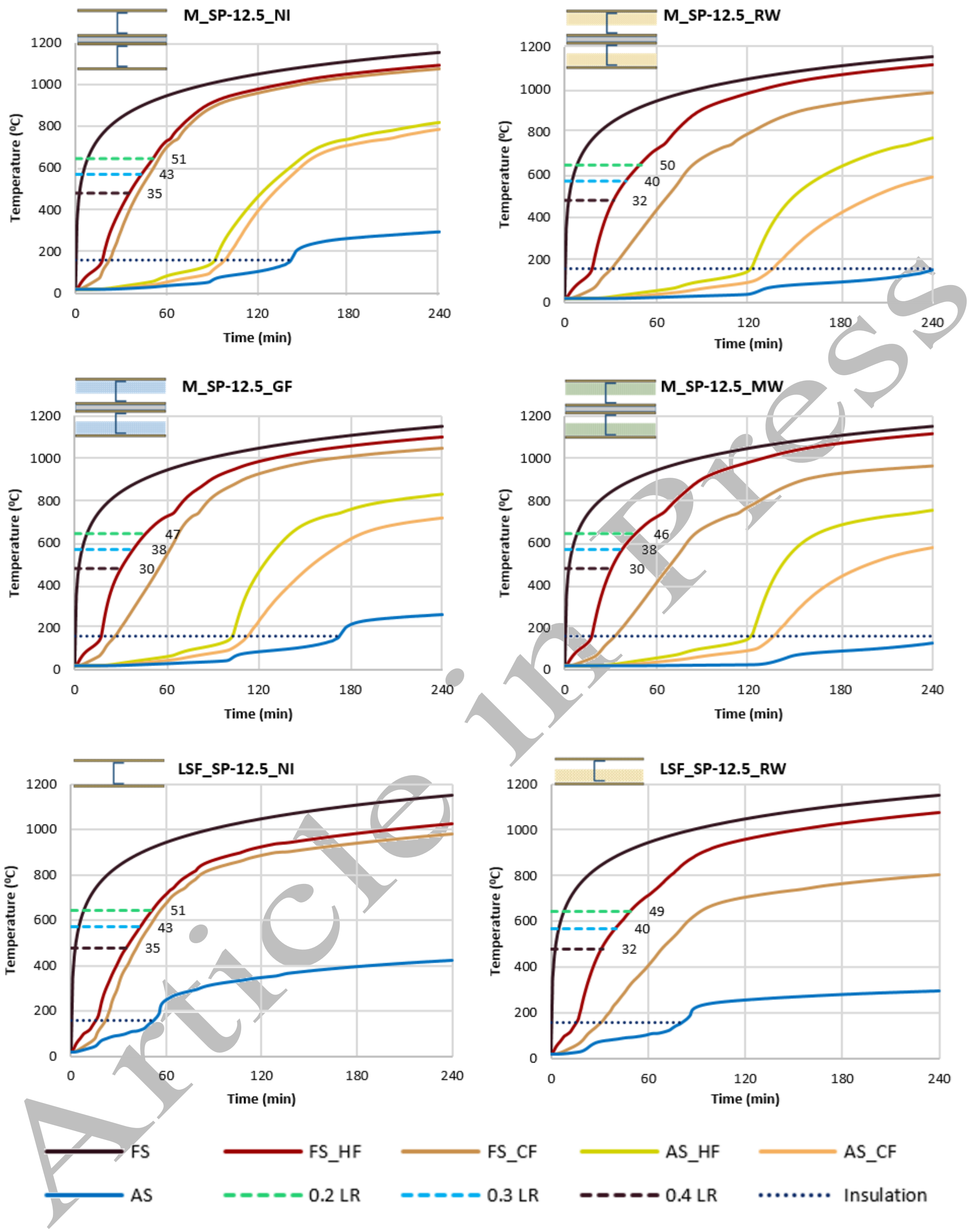

Figure 17: Heat transfer analysis results for 12.5mm thick single plasterboard walls

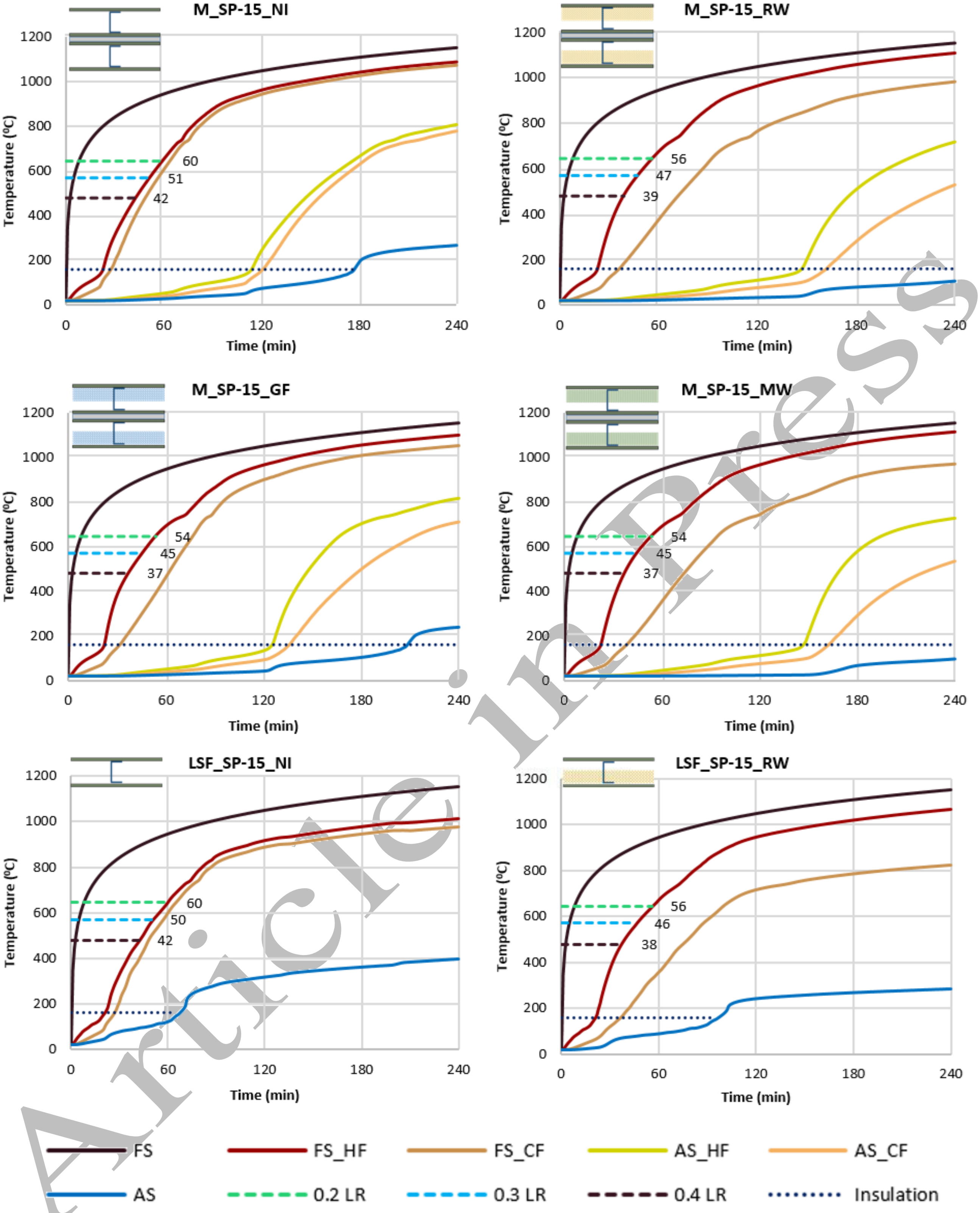

Figure 18: Heat transfer analysis results of 15 mm thick single plasterboard walls

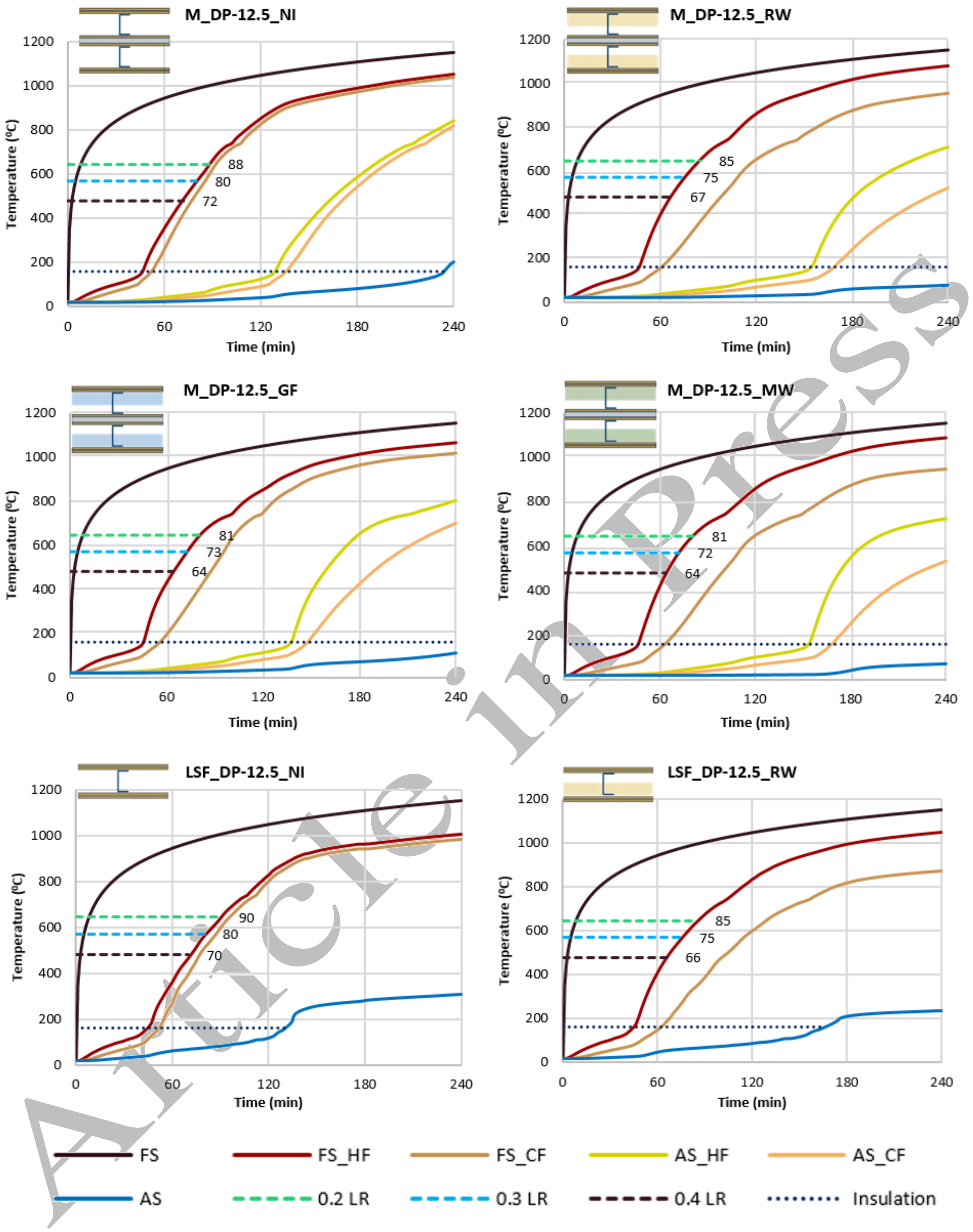

Figure 19: Heat transfer analysis results of 12.5mm thick double plasterboard walls

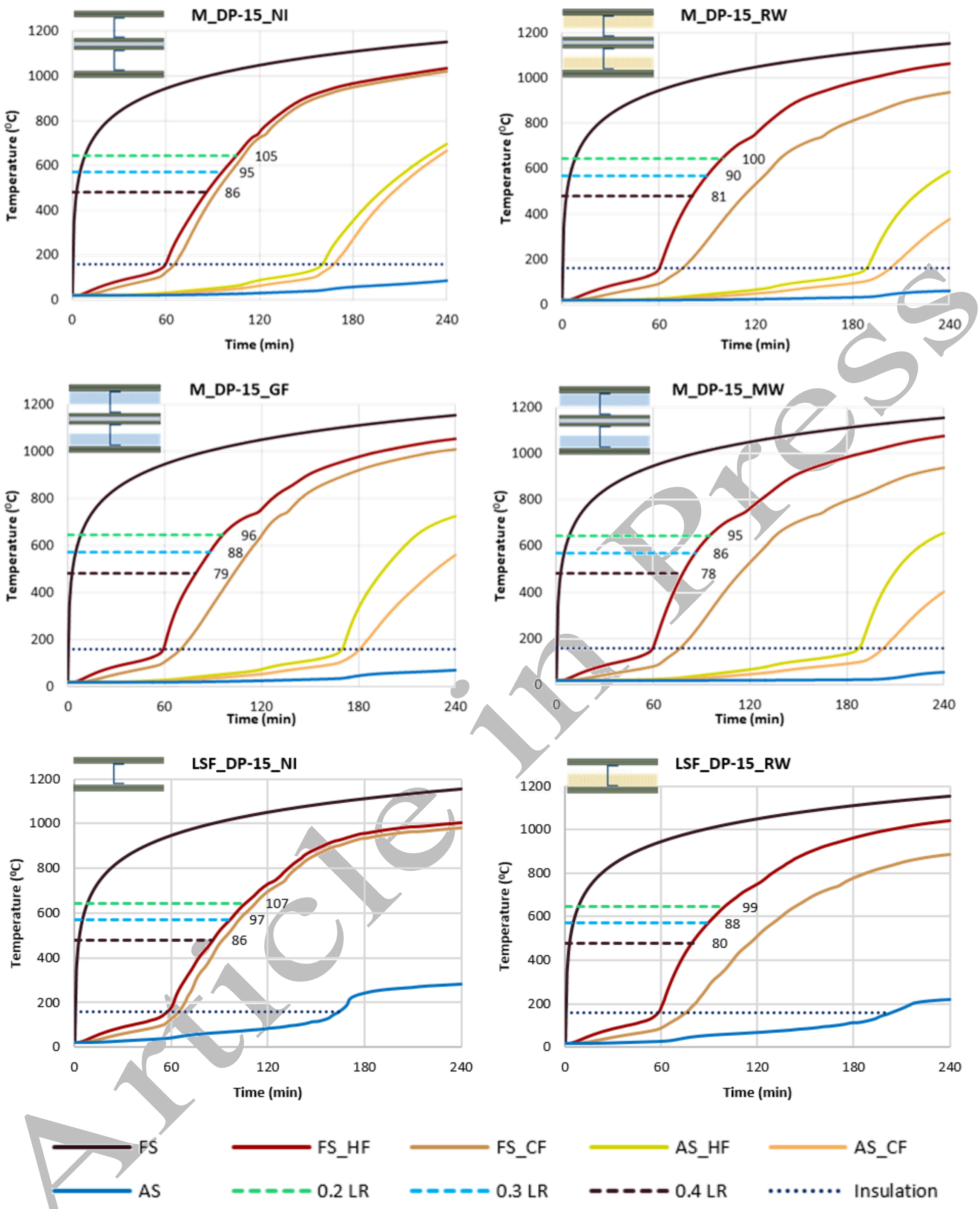

Figure 20: Heat transfer analysis results of 15 mm thick double plasterboard walls

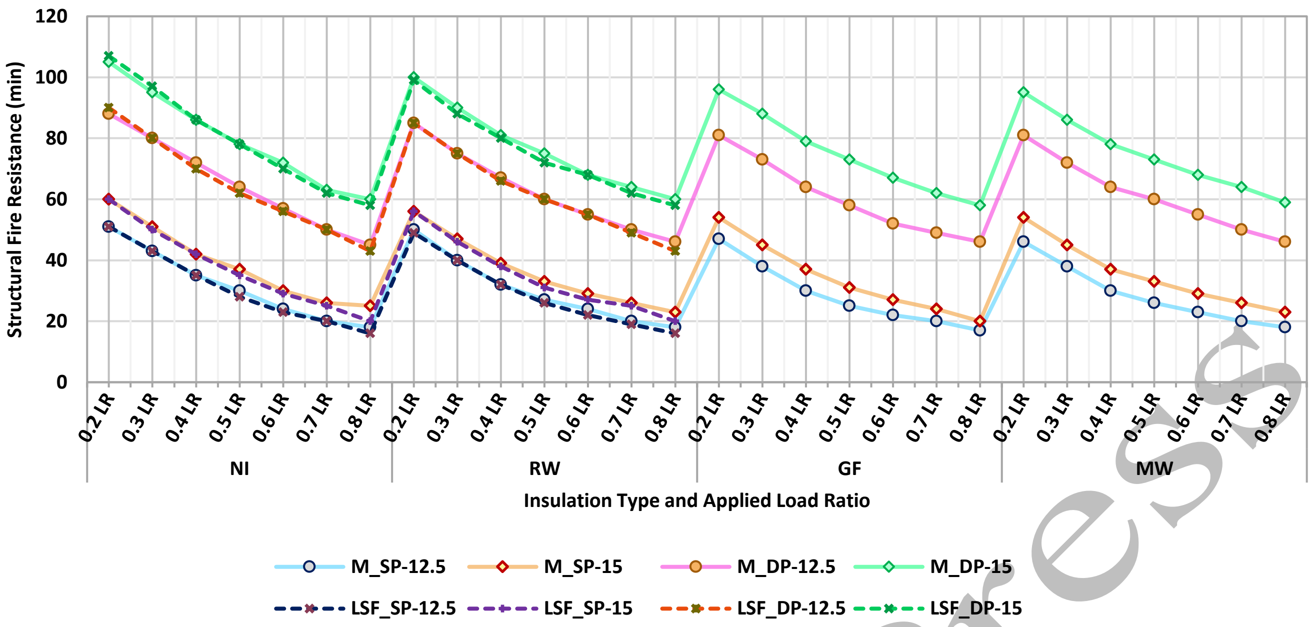

Figure 21: Structural fire resistances of modular and LSF wall panels

The structural FRL at different LR values for the modular and LSF walls have been graphed in Figure 21. When analysing the results, wall specimens without any cavity insulation demonstrate slightly increased structural fire-resistant times than the wall specimens with insulation. This behaviour can be explained from the time variant temperature contours of non-insulated and insulated wall specimens as described in section 3.5. Insulation material inside a LSF wall panel leads to increased HF temperature, hence at a certain LR the HF temperature of an insulated wall panel would reach earlier than that of the related non-insulated wall panel, meaning the FRL of the insulated wall panel is less than the latter one. Yet, when the LR value is greater than 0.7 the FRL has not reduced in the insulated panels because the FRLs are comparatively smaller when LR is higher and during the initial stage the heat absorption rate of the insulation material is much higher. Therefore, approximately up to 30 minutes HF temperatures of the insulated wall panels are slightly reduced than the non-insulated walls.

Another prominent observation is that the insulation material option, from rock wool to glass fibre or from glass fibre to mineral wool has no noticeable influence on the structural fire resistance. The densities and the thermal conductivities of the three considered insulation types indicated significant variation while the specific heats are in the same range. Therefore, HF temperature which drives the structural FRL would not be significantly affected by the insulation type while temperature profiles beneath the insulation layer (i.e. CF, AS) would be. In that case the insulation FRL of walls are influenced by the insulation type. However, since most of the insulated wall panels demonstrate more than 240 minutes insulation FRL which is the maximum FRL practiced in the current design practice.

Most interestingly, the structural fire resistance of modular LSF wall panels have been critically coincided with the corresponding LSF wall arrangements. On contrary, the insulation fire resistance between LSF wall and corresponding modular LSF wall panel has a significant difference. This result confirms that from single skin to double skin LSF walls, there is no significant effect on the critical HF temperature. Therefore, when determining the structural FRL of a modular LSF wall, it is appropriate to use a single skin LSF wall for the experimental or numerical analysis. However, time dependent temperature profiles of CF and AS is significantly reduced in the double skin LSF walls with respect to the single skin LSF walls. Hence, testing of single skin LSF walls for insulation failure instead of double skin or modular LSF walls, is not an acceptable approach.

Specifically, in single plasterboard arrangements, the insulation fire resistance of modular LSF wall panels are 170% greater than that of the mapped LSF wall specimens, while in double plasterboard arrangements the insulation fire resistance increment of modular LSF wall panels is 50% to 80%.

The guidelines on FRL of building component with respect to the AS/NZS: 4600:2018 [57], directs to use 30 minutes time steps. Hence, the FRL values for the wall panels have been calculated at different LRs. Therefore, the proposed FRL in structural and insulation criteria for the parametric wall specimens are presented in Table 6.

Table 6: Proposed FRL for modular and LSF wall specimens at different LRs

Wall Type	Load Ratio	Fire Resistance for different Insulation Options (min)			
		NI	RW	GF	MW
M_SP-12.5	NLB	-/-/120	-/-/240	-/-/150	-/-/240
	0.2	30/-/120	30/-/240	30/-/150	30/-/240
	0.3	30/-/120	30/-/240	30/-/150	30/-/240
	0.4	30/-/120	30/-/240	30/-/150	30/-/240
	0.5	30/-/120	-/-/240	-/-/150	-/-/240
	0.6	-/-/120	-/-/240	-/-/150	-/-/240
	0.7	-/-/120	-/-/240	-/-/150	-/-/240
	0.8	-/-/120	-/-/240	-/-/150	-/-/240
LSF_SP-12.5	NLB	-/-/30	-/-/60		
	0.2	30/-/30	30/-/60		
	0.3	30/-/30	30/-/60		
	0.4	30/-/30	30/-/60		
	0.5	-/-/30	-/-/60		
	0.6	-/-/30	-/-/60		
	0.7	-/-/30	-/-/60		
	0.8	-/-/30	-/-/60		
M_SP-15	NLB	-/-/150	-/-/240	-/-/240	-/-/240
	0.2	60/-/150	30/-/240	30/-/240	30/-/240
	0.3	30/-/150	30/-/240	30/-/240	30/-/240
	0.4	30/-/150	30/-/240	30/-/240	30/-/240
	0.5	30/-/150	30/-/240	30/-/240	30/-/240
	0.6	30/-/150	-/-/240	-/-/240	-/-/240
	0.7	-/-/150	-/-/240	-/-/240	-/-/240

	0.8	-/-/150	-/-/240	-/-/240	-/-/240
LSF_SP-15	NLB	-/-/60	-/-/90		
	0.2	60/-/60	30/-/90		
	0.3	30/-/60	30/-/90		
	0.4	30/-/60	30/-/90		
	0.5	30/-/60	30/-/90		
	0.6	-/-/60	-/-/90		
	0.7	-/-/60	-/-/90		
	0.8	-/-/60	-/-/90		
M_DP-12.5	NLB	-/-/210	-/-/240	-/-/240	-/-/240
	0.2	60/-/210	60/-/240	60/-/240	60/-/240
	0.3	60/-/210	60/-/240	60/-/240	60/-/240
	0.4	60/-/210	60/-/240	60/-/240	60/-/240
	0.5	60/-/210	60/-/240	30/-/240	60/-/240
	0.6	30/-/210	30/-/240	30/-/240	30/-/240
	0.7	30/-/210	30/-/240	30/-/240	30/-/240
	0.8	30/-/210	30/-/240	30/-/240	30/-/240
LSF_DP-12.5	NLB	-/-/120	-/-/150		
	0.2	90/-/120	60/-/150		
	0.3	60/-/120	60/-/150		
	0.4	60/-/120	60/-/150		
	0.5	60/-/120	60/-/150		
	0.6	30/-/120	30/-/150		
	0.7	30/-/120	30/-/150		
	0.8	30/-/120	30/-/150		
M_DP-15	NLB	-/-/240	-/-/240	-/-/240	-/-/240
	0.2	90/-/240	90/-/240	90/-/240	90/-/240
	0.3	90/-/240	90/-/240	60/-/240	60/-/240
	0.4	60/-/240	60/-/240	60/-/240	60/-/240
	0.5	60/-/240	60/-/240	60/-/240	60/-/240
	0.6	60/-/240	60/-/240	60/-/240	60/-/240
	0.7	60/-/240	60/-/240	60/-/240	60/-/240
	0.8	60/-/240	60/-/240	30/-/240	30/-/240
LSF_DP-15	NLB	-/-/150	-/-/180		
	0.2	90/-/150	90/-/180		
	0.3	90/-/150	60/-/180		
	0.4	60/-/150	60/-/180		
	0.5	60/-/150	60/-/180		
	0.6	60/-/150	60/-/180		
	0.7	60/-/150	60/-/180		
	0.8	30/-/150	30/-/180		

Notes:

M – Modular LSF wall panel

LSF – Light-gauge Steel Frame Wall

SP – Single Plasterboard

DP – Double Plasterboard

NLB – Non-loadbearing walls

Load Ratio (LR) – The ratio between the applied load on the LSF wall with respect to its load bearing capacity at the ambient temperature

FRL – Fire Resistance Level

However, the above method can be way more conservative due to rounding-down the fire resistance to the nearest 30 minutes step. Therefore, another innovative approach was followed, where the LR values were back calculated to obtain required FRLs. As shown in Table 7, the HF temperatures at the required FRLs were first evaluated from HTA. Then that HF temperature was considered as the critical HF temperature to determine the corresponding LR from Figure 15. The LR calculated this way, will be the maximum applicable LR to assert the required FRL chosen at the initial stage. When it comes to the designing stage, approach used in Table 7 is the most appropriate method to determine the maximum applicable LR to achieve a specified FRL.

Table 7: Maximum applicable LR to obtain required FRL

Wall Type	Insulation Type	Hot Flange Temperature (^{0}C) at				Maximum Applicable Load Ratio at			
		30 minutes	60 minutes	90 minutes	120 minutes	30 minutes	60 minutes	90 minutes	120 minutes
M_SP-12.5	NI	408	729	913	977	0.50	<0.10	<0.10	<0.10
	RW	453	720	907	982	0.45	<0.10	<0.10	<0.10
	GF	479	726	906	986	0.42	<0.10	<0.10	<0.10
	MW	474	725	905	983	0.42	<0.10	<0.10	<0.10
LSF_SP-12.5	NI	421	716	867	925	0.48	0.10	<0.10	<0.10
	RW	466	714	890	960	0.43	0.10	<0.10	<0.10
M_SP-15	NI	314	654	878	963	0.60	0.17	<0.10	<0.10
	RW	340	676	864	964	0.57	0.14	<0.10	<0.10
	GF	384	692	864	965	0.52	0.12	<0.10	<0.10
	MW	361	691	860	965	0.55	0.12	<0.10	<0.10
LSF_SP-15	NI	331	648	852	919	0.58	0.18	<0.10	<0.10
	RW	374	673	849	947	0.53	0.15	<0.10	<0.10
M_DP-12.5	NI	102	357	665	854	0.90	0.55	0.16	<0.10
	RW	101	401	686	861	0.90	0.50	0.13	<0.10
	GF	104	429	703	850	0.90	0.47	0.11	<0.10
	MW	102	422	702	858	0.90	0.48	0.11	<0.10
LSF_DP	NI	107	364	643	830	0.90	0.54	0.19	<0.10

-12.5	RW	105	414	676	835	0.90	0.49	0.14	<0.10
M_DP-15	NI	85	164	520	751	0.93	0.80	0.37	<0.10
	RW	84	160	573	756	0.93	0.81	0.29	<0.10
	GF	88	180	593	755	0.92	0.78	0.26	<0.10
	MW	86	164	608	763	0.93	0.80	0.25	<0.10
LSF_DP-15	NI	89	177	521	728	0.92	0.78	0.36	<0.10
	RW	88	190	579	751	0.92	0.76	0.29	<0.10

The LR values less than 0.2, practically has no significance because the minimum LR practiced in the industry is 0.2. Also for design convention the LR values have been round down to the nearest 0.05 in this study. As a result the proposed maximum LRs for 30 minutes, 60 minutes and 90 minutes FRL has been proposed in Table 8.

Table 8: Proposed safe LRs to obtain required FRL

Wall Type	Insulation Type	Proposed Load Ratios to obtain required FRL		
		30 minutes	60 minutes	90 minutes
M_SP-12.5	NI	0.45	-	-
	RW	0.40	-	-
	GF	0.40	-	-
	MW	0.40	-	-
LSF_SP-12.5	NI	0.45	-	-
	RW	0.40	-	-
M_SP-15	NI	0.55	-	-
	RW	0.55	-	-
	GF	0.50	-	-
	MW	0.50	-	-
LSF_SP-15	NI	0.55	-	-
	RW	0.50	-	-
M_DP-12.5	NI	0.85	0.55	-
	RW	0.90	0.50	-
	GF	0.85	0.45	-
	MW	0.85	0.45	-
LSF_DP-12.5	NI	0.85	0.50	-
	RW	0.85	0.45	-
M_DP-15	NI	0.90	0.80	0.35
	RW	0.90	0.80	0.25
	GF	0.90	0.75	0.25
	MW	0.90	0.80	0.20
LSF_DP-15	NI	0.90	0.75	0.35
	RW	0.90	0.75	0.25

5 Conclusion

This work has presented the numerical study on modular LSF wall panels and results. Validated numerical models with fire tests were used to investigate the fire performance of modular LSF wall panels with different configurations. In total, 16 different types of modular LSF wall panel configurations were subjected for the investigation under standard fire condition. The LSF modular LSF wall types vary in terms of the number of plasterboard linings, plasterboard thickness, insulation material. Based on the results following conclusions can be drawn:

- Developed heat transfer numerical models showed a good agreement with fire test time-temperature profiles. Thus, numerical models are an effective tool to predict the fire resistance time of Modular LSF wall panels.
- The structural failure times of the modular LSF wall panels were obtained from established LR vs HF relationship and no noticeable difference was obtained for a particular modular LSF wall panel with different insulation materials, since the type of insulation material has hardly influenced the HF temperature of the wall. Yet, there are some noticeable changes in terms of insulation failure time over the type of insulation.
- Furthermore, from single to double skin LSF wall structures, the critical HF temperature variation is barely varied. Therefore, there is no noticeable difference in the structural fire resistance time between the modular LSF wall panels and the corresponding mapped LSF wall configurations.
- Modular LSF wall panels experience up to 170% higher insulation fire rating for single-lined plasterboards and up to 80 % higher insulation fire rating for double-lined plasterboard configurations compared to the mapped conventional LSF wall configuration.

6 Acknowledgement

The authors would like to acknowledge the ESS Modular Limited., Northumbria University and University of Sri Jayawardenepura for the financial support and research facilities.

References

[1] R. M. Lawson, R. G. Ogden, and R. Bergin, "Application of Modular Construction in High-Rise Buildings," *Journal of Architectural Engineering*, vol. 18, no. 2, pp. 148-154, 2012, doi: 10.1061/(asce)ae.1943-5568.0000057.

[2] W. Ferdous, Y. Bai, T. D. Ngo, A. Manalo, and P. Mendis, "New advancements, challenges and opportunities of multi-storey modular buildings – A state-of-the-art review," *Engineering Structures*, vol. 183, pp. 883-893, 2019/03/15/ 2019, doi: https://doi.org/10.1016/j.engstruct.2019.01.061.

[3] A. W. Lacey, W. Chen, H. Hao, and K. Bi, "Structural response of modular buildings – An overview," *Journal of Building Engineering*, vol. 16, pp. 45-56, 2018, doi: 10.1016/j.jobe.2017.12.008.

[4] G. Perampalam, R. Dobson, K. Poologanathan, K. D. Tsavdaridis, B. Nagaratnam, and E. Iacovidou, "Modular Building Design: Post-Brexit Housing," *ce/papers*, vol. 3, no. 3-4, pp. 219-224, 2019, doi: 10.1002/cepa.1160.

[5] W. Wendy and B. Cassie, "Tackling the under-supply of housing in England," House of Commons, Briefing Paper 2020. [Online]. Available: https://researchbriefings.files.parliament.uk/documents/CBP-7671/CBP-7671.pdf

[6] "Smart construction: How offsite manufacturing can transform our industry," KPMG, 2016. [Online]. Available: https://assets.kpmg/content/dam/kpmg/pdf/2016/04/SmartConstructionReport.pdf

[7] Y. Dias, P. Keerthan, and M. Mahendran, "Predicting the fire performance of LSF walls made of web stiffened channel sections," *Engineering Structures*, vol. 168, pp. 320-332, 2018/08/01/ 2018, doi: https://doi.org/10.1016/j.engstruct.2018.04.072.

[8] S. Kesawan and M. Mahendran, "Fire tests of load-bearing LSF walls made of hollow flange channel sections," *Journal of Constructional Steel Research*, vol. 115, pp. 191-205, 2015/12/01/ 2015, doi: https://doi.org/10.1016/j.jcsr.2015.07.020.

[9] M. Rusthi, A. D. Ariyanayagam, and M. Mahendran, "Fire design of LSF wall systems made of web-stiffened lipped channel studs," *Thin-Walled Structures*, vol. 127, pp. 588-603, 2018/06/01/ 2018, doi: https://doi.org/10.1016/j.tws.2018.02.020.

[10] W. Chen, J. Ye, and X. Li, "Fire experiments of cold-formed steel non-load-bearing composite assemblies lined with different boards," *Journal of Constructional Steel Research*, vol. 158, pp. 290-305, 2019/07/01/ 2019, doi: https://doi.org/10.1016/j.jcsr.2019.04.003.

[11] Y. Dias, P. Keerthan, and M. Mahendran, "Fire performance of steel and plasterboard sheathed non-load bearing LSF walls," *Fire Safety Journal*, vol. 103, pp. 1-18, 2019/01/01/ 2019, doi: https://doi.org/10.1016/j.firesaf.2018.11.005.

[12] S. Gnanachelvam, A. Ariyanayagam, and M. Mahendran, "Fire resistance of light gauge steel framed wall systems lined with PCM-plasterboards," *Fire Safety Journal*, vol. 108, p. 102838, 2019/09/01/ 2019, doi: https://doi.org/10.1016/j.firesaf.2019.102838.

[13] P. Keerthan and M. Mahendran, "Thermal Performance of Composite Panels Under Fire Conditions Using Numerical Studies: Plasterboards, Rockwool, Glass Fibre and Cellulose Insulations," *Fire Technology*, vol. 49, no. 2, pp. 329-356, 2013/04/01 2013, doi: 10.1007/s10694-012-0269-6.

[14] M. Rusthi, A. Ariyanayagam, M. Mahendran, and P. Keerthan, "Fire tests of Magnesium Oxide board lined light gauge steel frame wall systems," *Fire Safety Journal*, vol. 90, pp. 15-27, 2017/06/01/ 2017, doi: https://doi.org/10.1016/j.firesaf.2017.03.004.

[15] A. D. Ariyanayagam and M. Mahendran, "Fire tests of non-load bearing light gauge steel frame walls lined with calcium silicate boards and gypsum plasterboards," *Thin-Walled Structures*, vol. 115, pp. 86-99, 2017/06/01/ 2017, doi: https://doi.org/10.1016/j.tws.2017.02.005.

[16] L. Kristanto, H. Sugiharto, S. W. D. Agus, and S. A. Pratama, "Calcium Silicate Board as Wall-facade," *Procedia Engineering*, vol. 171, pp. 679-688, 2017/01/01/ 2017, doi: https://doi.org/10.1016/j.proeng.2017.01.409.

[17] D. Perera *et al.*, "Fire Performance of Cold, Warm and Hybrid LSF Wall Panels Using Numerical Studies," *Thin-Walled Structures*, 2020.

[18] J. Jing, G. C. Clifton, K. Roy, and J. B. P. Lim, "Three-storey modular steel building with a novel slider device: Shake table tests on a scaled down model and numerical investigation," *Thin-Walled Structures*, vol. 155, p. 106932, 2020/10/01/ 2020, doi: https://doi.org/10.1016/j.tws.2020.106932.

[19] J. Jing, G. Charles Clifton, K. Roy, and J. B. P. Lim, "Performance of a novel slider device in multi-storey cold-formed steel modular buildings under seismic loading," *Structures*, vol. 27, pp. 212-246, 2020/10/01/ 2020, doi: https://doi.org/10.1016/j.istruc.2020.05.051.

[20] J. Jing, G. C. Clifton, K. Roy, and J. B. P. Lim, "Seismic protection of modular buildings with bonded rubber unit sliders: Experimental study," *Thin-Walled Structures*, vol. 154, p. 106790, 2020/09/01/ 2020, doi: https://doi.org/10.1016/j.tws.2020.106790.

[21] R. Lawson, A. Way, M. Heywood, J. Lim, R. Johnston, and K. Roy, "Stability of light steel walls in compression with plasterboards on one or both sides," *Proceedings of the Institution of Civil Engineers - Structures and Buildings*, vol. 173, pp. 1-61, 01/25 2019, doi: 10.1680/jstbu.18.00118.

[22] M. Feng and Y. C. Wang, "An experimental study of loaded full-scale cold-formed thin-walled steel structural panels under fire conditions," *Fire Safety Journal*, vol. 40, no. 1, pp. 43-63, 2005/02/01/ 2005, doi: https://doi.org/10.1016/j.firesaf.2004.08.002.

[23] M. Feng, Y. C. Wang, and J. M. Davies, "Axial strength of cold-formed thin-walled steel channels under non-uniform temperatures in fire," *Fire Safety Journal*, vol. 38, no. 8, pp. 679-707, 2003/12/01/ 2003, doi: https://doi.org/10.1016/S0379-7112(03)00070-5.

[24] K. Roy *et al.*, "Collapse behaviour of a fire engineering designed single-storey cold- formed steel building in severe fires," *Thin-Walled Structures*, vol. 142, pp. 340-357, 2019/09/01/ 2019, doi: https://doi.org/10.1016/j.tws.2019.04.046.

[25] W. Chen, J. Jiang, J. Ye, Q. Zhao, K. Liu, and C. Xu, "Thermal behavior of external-insulated cold-formed steel non-load-bearing walls exposed to different fire conditions," *Structures*, vol. 25, pp. 631-645, 2020/06/01/ 2020, doi: https://doi.org/10.1016/j.istruc.2020.03.044.

[26] N. Degtyareva, P. Gatheeshgar, K. Poologanathan, S. Gunalan, K. D. Tsavdaridis, and S. Napper, "New distortional buckling design rules for slotted perforated cold-formed steel beams," *Journal of Constructional Steel Research*, vol. 168, 2020, doi: 10.1016/j.jcsr.2020.106006.

[27] N. Degtyareva, P. Gatheeshgar, P. Keerthan, S. Gunalan, I. Shyha, and A. McIntosh, "Local buckling strength and design of cold-formed steel beams with slotted perforations," *Thin-Walled Structures*, vol. (In press), 2020.

[28] N. Degtyareva, P. Gatheeshgar, K. Poologanathan, S. Gunalan, M. Lawson, and P. Sunday, "Combined bending and shear behaviour of slotted perforated steel channels: Numerical studies," *Journal of Constructional Steel Research*, vol. 161, pp. 369-384, 2019, doi: 10.1016/j.jcsr.2019.07.008.

[29] P. Gatheeshgar, P. Keerthan, G. Shanmuganathan, T. Konstantinos Daniel, N. Brabha, and I. Eleni, "Optimised cold-formed steel beams in modular building applications," *Journal of Building Engineering*, vol. (In press), 2020.

[30] R. M. Lawson, "Light Steel Modular Construction," in "Technical Information Sheet ED014," The Steel Construction Institute, 2012.

[31] R. M. Lawson and A. G. J. Way, "Fire Safety of Light Steel Construction," in "Technical Information Sheet ED016," The Steel Construction Institute, 2012.

[32] C. Chris and M. Hans J. "Emergency services / Investigation underway after huge fire destroys Moorfield Hotel." Shetland News. https://www.shetnews.co.uk/2020/07/27/investigation-underway-after-huge-fire-destroys-moorfield-hotel/ (accessed 03/08/2020.

[33] P. Apps. "Are two fire on the Shetland Islands a canary in the coal mine for modular construction?" Insde Housing. https://www.insidehousing.co.uk/insight/insight/are-two-fires-on-the-shetland-islands-a-canary-in-the-coal-mine-for-modular-construction (accessed 2021).

[34] O.Vassart, B.Zhao, L.G.Cajot, F.Robert, U.Meyer, and A.Frangi, "JRC Science and Policy Reports," in "Eurocodes: Background & Applications Structural Fire Design," European Union, Luxembourg: Publications Office of the European Union, EUR 26698 EN 2014. [Online]. Available:

https://ec.europa.eu/jrc

[35] M. Bellová, "EUROCODES: Structural Fire Design," *Procedia Engineering*, vol. 65, pp. 382-386, 2013/01/01/ 2013, doi: https://doi.org/10.1016/j.proeng.2013.09.059.

[36] *Methods for fire tests on building materials, components and structures*, ISBN 978 1 74342 918 1, F. S. Committee FP-018, 2014 2014.

[37] *ISO 13784-1:2014 Reaction to fire test for sandwich panel building systems*, I. O. f. Standards, 2014.

[38] *BS EN 13501-1:2018 Fire classsification of construction products and building elements.*, B. S. Institution, London, UK, 2018.

[39] *Cold-Formed Steel Design Manual*, A. I. a. S. Institute, Washington, D.C., 2017.

[40] V. Babrauskas and R. B. Williamson, "The historical basis of fire resistance testing — Part II," *Fire Technology*, vol. 14, no. 4, pp. 304-316, 1978/11/01 1978, doi: 10.1007/BF01998390.

[41] J. F. Nyman, "Equivalent Fire Resistance Ratings of Construction Elements Exposed to Realistic Fires," 2002.

[42] T. Lennon and D. Moore, "The natural fire safety concept—full-scale tests at Cardington," *Fire Safety Journal*, vol. 38, no. 7, pp. 623-643, 2003/11/01/ 2003, doi: https://doi.org/10.1016/S0379-7112(03)00028-6.

[43] B. Nagy and E. Tóth, "Finite Element Analysis of Composite Ceramic-Concrete Slab Constructions Exposed to Fire," *Applied Mechanics and Materials*, vol. 861, pp. 88-95, 12/05 2016, doi: 10.4028/www.scientific.net/AMM.861.88.

[44] *Eurocode 3: Design of steel structures - Part 1-2: General rules - Structural fire design*, T. E. Union, 23 April 2004 2005.

[45] S. Gunalan, P. Kolarkar, and M. Mahendran, "Experimental study of load bearing cold-formed steel wall systems under fire conditions," *Thin-Walled Structures*, vol. 65, pp. 72-92, 2013/04/01/ 2013, doi: https://doi.org/10.1016/j.tws.2013.01.005.

[46] H. Magarabooshanam, A. Ariyanayagam, and M. Mahendran, "Fire resistance of non-load bearing LSF walls with varying cavity depth," *Thin-Walled Structures*, vol. 150, p. 106675, 2020/05/01/ 2020, doi: https://doi.org/10.1016/j.tws.2020.106675.

[47] S. Gunalan and M. Mahendran, "Fire performance of cold-formed steel wall panels and prediction of their fire resistance rating," *Fire Safety Journal*, vol. 64, pp. 61-80, 2014/02/01/ 2014, doi: https://doi.org/10.1016/j.firesaf.2013.12.003.

[48] W. Chen, J. Ye, Y. Bai, and X.-L. Zhao, "Improved fire resistant performance of load bearing cold-formed steel interior and exterior wall systems," *Thin-Walled Structures*, vol. 73, pp. 145-157, 2013/12/01/ 2013, doi: https://doi.org/10.1016/j.tws.2013.07.017.

[49] S. Gunalan, "Structural Behaviour and Design of Cold-formed Steel Wall Systems under Fire Conditions," Doctor of Philosophy, School of Urban Development, Faculty of Environment and Engineering, Quinsland University of Technology, 2011.

[50] A. D. Ariyanayagam and M. Mahendran, "Fire performance of load bearing LSF wall systems made of low strength steel studs," *Thin-Walled Structures*, vol. 130, pp. 487-504, 2018/09/01/ 2018, doi: https://doi.org/10.1016/j.tws.2018.05.018.

[51] J. C. Nagetgaal, "Computer process for prescribing second-order tetrahedral elements during deformation simulation in the design analysis of structures," ed: Google Patents, 2004.

[52] M. Rusthi, P. Keerthan, M. Mahendran, and A. Ariyanayagam, "Investigating the fire performance of LSF wall systems using finite element analyses," *Journal of Structural Fire Engineering*, vol. 8, no. 4, pp. 354-376, 2017, doi: 10.1108/jsfe-04-2016-0002.

[53] H. Wang, "Heat transfer analysis of components of construction exposed to fire," PhD, Department

of Civil Engineering and Construction, University of Salford, 1995. [Online]. Available: http://usir.salford.ac.uk/id/eprint/14780/

[54] F. Liu, F. Fu, Y. Wang, and Q. Liu, "Fire performance of non-load-bearing light-gauge slotted steel stud walls," *Journal of Constructional Steel Research*, vol. 137, pp. 228-241, 2017/10/01/ 2017, doi: https://doi.org/10.1016/j.jcsr.2017.06.034.

[55] D. Simulia. "ABAQUS Analysis User's Manual." https://classes.engineering.wustl.edu/2009/spring/mase5513/abaqus/docs/v6.6/books/stm/default.htm?startat=ch02s11ath45.html (accessed 2020).

[56] P. Keerthan and M. Mahendran, "Numerical studies of gypsum plasterboard panels under standard fire conditions," *Fire Safety Journal*, vol. 53, pp. 105-119, 2012/10/01/ 2012, doi: https://doi.org/10.1016/j.firesaf.2012.06.007.

[57] Joint Technical Committee BD-082, Ed. *Cold-formed steel structures* (Fire Design. Council of Standards Australia and New Zealand Standards, 2018.